CONTRACTOR REPORT

SAND87—7025
Unlimited Release
UC—236

Liquid Metal Thermal-Electric Converter Electrode Development

J. I. Martinez, Editor
Sandia National Laboratories
Division 6227
Albuquerque, NM 87185

Prepared by Sandia National Laboratories Albuquerque, New Mexico 87185 and Livermore California 94550 for the United States Department of Energy under Contract DE-AC04-76DP00789

Printed February 1988

DISCLAIMER

Printed in the United States of America
Available from
National Technical Information Service
U.S. Department of Commerce
5285 Port Royal Road
Springfield, VA 22161

NTIS price codes
Printed copy: A04
Microfiche copy: A01

Distribution
Category UC-236

SAND87-7025
Unlimited Release
Printed February 1988

SAND--87-7025

DE88 009252

Liquid Metal Thermal-Electric Converter Electrode Development

J. I Martinez, Editor
Division 6227
Sandia National Laboratories
Albuquerque, NM 87185

Sandia Contract 64-9358

ABSTRACT

This report describes work done in support of distributed receiver technology development. Dish-electric systems are being pursued in an effort to circumvent the need for energy transport by providing for heat-to-electricity energy conversion by individual heat engines at the focal point of parabolic dish concentrators. The Liquid Metal Thermal-Electric Converter is an engine that can convert thermal energy to electricity without the need for moving parts. The report documents the results of contracted work in the development of a long-lifetime, high-performance electrode for LMTEC, including the materials prepared for it.

ACKNOWLEDGEMENTS

The research described in this report was performed under contract to Sandia National Laboratories, Albuquerque, New Mexico, and was supported by the U. S. Department of Energy. The work described in Sections IV and VII was also supported in part by the U.S. Army Tank - Automotive Command, Warren, Michigan, and NASA.

Table of Contents

page blank

SOLAR THERMAL TECHNOLOGY:

FOREWORD

The research and development program described in this document was conducted within the U.S. Department of Energy's (DOE) Solar Thermal Technology Program. The goal of the Solar Thermal Technology Program is to advance the engineering and scientific understanding of solar thermal technology and to establish the technology base from which private industry can develop solar thermal power production options for introduction into the competitive energy market.

Solar thermal technology concentrates solar radiation by means of tracking mirrors or lenses onto a receiver where the solar energy is absorbed as heat and converted into electricity or incorporated into products as process heat. The two primary solar thermal technologies, central receivers and distributed receivers, employ various point and line-focus optics to concentrate sunlight. Current central reciever systems use fields of heliostats (two-axis tracking mirrors) to focus the sun's radiant energy onto a single tower-mounted receiver. Two approaches are predominant for distributed receivers. One approach is to use parabolic dishes up to 17 meters in diameter to track the sun in two axes and use mirrors or Fresnel lenses to focus radiant energy onto a receiver. Another approach is to use troughs and bowls as line-focus tracking reflectors to concentrate sunlight onto receiver tubes along their focal lines. Concentrating collector modules can be used alone or in a multi-module system. The concentrated radiant energy absorbed by the solar thermal recever is transported to the conversion process by a circulating working fluid. Receiver temperatures range from 100^{o}C in

low-temperature troughs to over 1500^{o} in dish and central receiver systems.

The Solar Thermal Technology Program is directing efforts to advance and improve promising system concepts through the research and development of solar thermal materials, components, and subsystems, and the testing and performance evaluation of subsystems and systems. These efforts are carried out through the technical direction of DOE and its network of national laboratories who work with private industry. Together they have established a comprehensive, goal-directed program to improve performance and provide technically proven options for eventual incorporation into the Nation's energy supply.

To be successful in contributing to an adequate national energy supply at reasonable cost, solar thermal energy must eventually be economically competitive with a variety of other energy sources. Components and system-level performance targets have been developed as quantitative program goals. The performance targets are used in planning research and development activities, measuring progress, assessing alternative technology options, and making optimal component developments. These targets will be pursued vigorously to ensure a successful program.

This report describes work done in support of distributed receiver technology development. Dish-electric systems are being pursued in an effort to circumvent the need for energy transport by providing for heat-to-electric energy conversion by individual heat engines at the focal point of parabolic dish concentrators. The Liquid Metal Thermal-Electric Converter (LMTEC) is an engine that can convert thermal energy to electricity without the need for moving parts. This concept represents the possibility for significant improvement in heat

engines since operation and maintenance costs will be inherently low. A Sandia-conducted study comparing presently available and long-term heat engines concluded that the LMTEC was one of the most promising technologies for dish-electric applications. This report documents the results of contracted work in the development of a long-lifetime, high-performance electrode for LMTEC. A high-performance electrode would significantly impact the development of the LMTEC, thus enhancing dish-electric systems.

page blank

SUMMARY

The Liquid Metal Thermal Electric Converter (LMTEC) is a new, high-efficiency (20 -40%), direct thermal-to-electric conversion device with the potential for low maintenance due to the absence of moving parts, as well as compactness and modularity. Since the high-temperature reservoir may be heated externally, the LMTEC may be coupled to chemical, nuclear, or solar heat sources. Its optimum operating temperature range (900 - 1300 K) makes it ideal for solar thermal applications using parabolic dish concentrators. The modularity of LMTEC units makes it possible for it to produce power efficiently over a range of concentrator sizes or power levels. The absence of moving parts implies low maintenance and quiet operation. The LMTEC's potentially high-power density of 0.5 kW/kg would minimize the volume and mass of the conversion system, thus reducing structural requirements. Before significant progress can be made in designing and testing LMTEC units, several technical questions must be answered. One of the most important issues is the acquisition of a long-life, high-power density, porous electrode. The objective addressed in this contract was to experimentally investigate new electrode materials and configurations with the intent of identifying high-power density electrodes with improved durability for possible solar thermal applications.

The mechanisms responsible for the observed performance of state-of-the-art molybdenum electrodes have been previously identified. The presence of sodium molybdate, a sodium ion conductor, in the pores of the electrode gives rise to ion transport enhancement and the resulting

high power densities. Initial degradation is primarily attributed to evaporation of the sodium molybdate from the pores. These studies were continued in this contract, and more details on the effects of sodium molybdate have been elucidated.

Electrodes were regenerated by the direct application of sodium molybdate, and this technique was found to change the electrodes' morphology as well as improve their performance. However, regeneration in this fashion has only limited potential in extending the operation of electrodes due to corrosion reactions that take place in the sodium molybdate/ molybdenum system. It is estimated that the lifetime for operation with satisfactory performance can be extended only to 1000 - 5000 hours. This range of lifetime would not be adequate for a system intended to operate over a 20-year minimum lifetime.

Very thin (<1 micron) film molybdenum electrodes with overlying current collection grids have shown promise to meet electrode performance goals without the aid of sodium molybdate as a sodium transport enhancer. Electrodes have exhibited high initial power densities (0.6 W/cm^2) comparable to fresh molybdenum electrodes. Although no lifetime data are yet available for these electrodes and they have not been optimized, these electrode compositions have characteristics that could result in long lifetime operation (>10,000 hours) in the 0.5 W/cm^2 range. Likewise, the platinum group-tungsten electrodes require further research in order to determine the mechanism of enhanced transport.

In conclusion, although significant progress has been made by this research on electrode technology, continued research remains to be done in this area before an electrode material as well as an application technique can be adapted for application on the inside of a beta" alumina tube as is require for the current LMTEC intended design.

I. INTRODUCTION

A. Background

The Liquid Metal Thermal Electric Converter (LMTEC) is a new device for high-efficiency direct conversion of thermal energy to electricity (1,2). The LMTEC accepts heat input in the range of 900 - 1300 K and rejects heat in the range of 400 - 800 K. Conversion efficiencies of 25 - 40% have been predicted (3), and an efficiency of 19% (4) and a power density of 1 W/cm^2 (3) have been reported. Its characteristics include: compactness (high power density), modularity, no moving parts, and omnifuel capability. Since the high-temperature liquid metal reservoir may be heated externally, the LMTEC may be coupled with chemical, nuclear, and solar heat sources. A comprehensive technical review of thermally regenerative electrochemical systems (5), carried out by the Solar Energy Research Institute (SERI) for the Department of Energy (DOE), found that the sodium heat engine (a LMTEC) has potentially the highest power density and efficiency of such systems. Thus, the characteristics and potential of the LMTEC make it a candidate for a variety of applications such as space and remote power (6,7), electric/hybrid vehicles (8), and terrestrial power generation from solar energy (9,10).

For solar thermal applications, the wide temperature range of the LMTEC is compatible with both parabolic dish concentrator as well as central reciever technologies. Since LMTEC parasitic losses scale

with electrode area and power output, the efficiency is relatively independent of size. Thus, modular units could be designed to produce efficient power generation over a range of concentrator sizes. Likewise, power levels could be reduced without large drops in efficiency during periods of low demand. In addition, the absence of moving parts should result in low maintenance and quiet operation. Finally, the heat rejection temperature of the LMTEC may make it suitable for coupling with a number of bottoming cycles which would yield even higher efficiency gains.

Preliminary solar energy systems projections were carried out by Subramanian and Hunt (9,10). They calculated that with a "near-term" LMTEC technology a parabolic dish concentrator system would achieve a converter/receiver efficiency of 25%, and with advanced technology 33%. In a possible LMTEC/Rankine cycle topping/bottoming system combination, estimated efficiencies would increase to 37% and 45% for the "near-term" and advanced-technology levels respectively. These efficiencies are very competitive with alternate technologies. No specific concept designs were developed in connection with these calculations, however. More recently, Sandia National Laboratories projections (11) based on new solar thermal concept designs and using a more rigorous approach, put LMTEC efficiencies in the 20 - 30% range depending on performance assumptions. Finally, it should be noted that the low-voltage, high-current characteristic of the LMTEC could be used for energy storage by the high-efficiency charging of batteries.

The operating cycle of the LMTEC is illustrated in Figure 1. A closed system is divided into a high-temperature/high-pressure region in contact with a heat source and a low-temperature/low-pressure region in conta : with a heat sink. These regions are separated by a barrier of

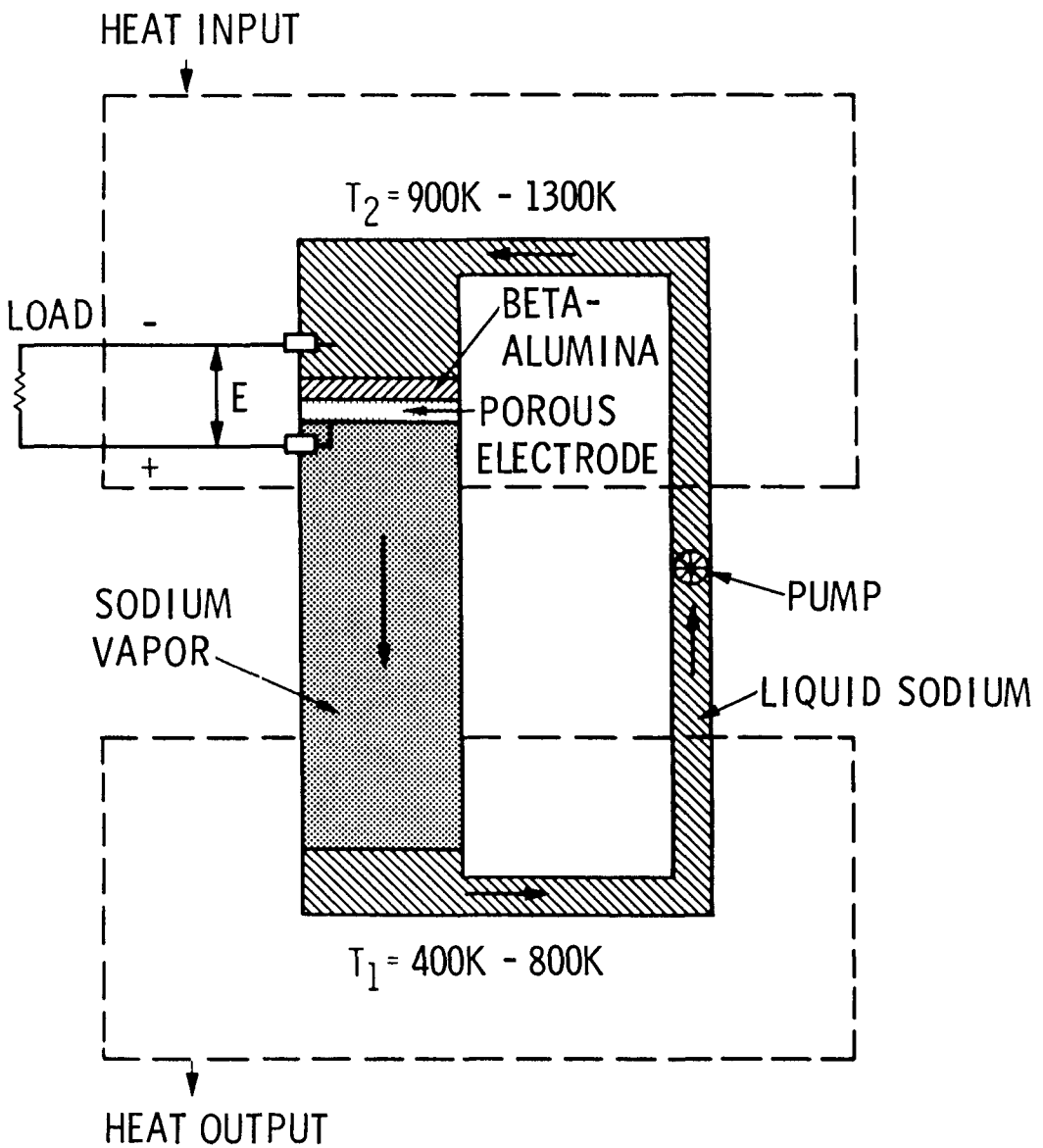

Figure 1. LMTEC Cycle Schematic.

beta"-alumina solid electrolyte (BASE) which has an ionic conductivity much larger than its electronic conductivity. The high temperature/high pressure region contains a liquid metal (e.g., molten sodium) at T_2 and the low-temperature/low-pressure region contains mostly metal vapor and a small amount of liquid metal at T_1. Electrical leads make contact with the positive, porous electrode that covers the low-pressure surface of the BASE and with the high-temperature liquid metal that constitutes the negative electrode. When the circuit is closed, metal ions are conducted through the BASE because of the difference in vapor pressures or chemical activity of the metal ions across the BASE, and the electrons flow to the porous electrode surface through the load, producing electrical work. The unique feature of the LMTEC cycle is that the metal is expanded nearly isothermally (within 50 K) through the BASE, causing the metal atoms to separate into metal ions and electrons. The LMTEC thus constitutes a unique system in which the work of isothermal expansion is coupled with ionization to produce electric power directly. A return line and an electromagnetic pump circulate the metal working fluid through the LMTEC. Further details on the LMTEC cycle may be found in references 1,2,3, and 6.

To achieve the benefits projected for a mature LMTEC technology, considerable research and development remain to be carried out. This report describes research results that address the principal technical issue associated with LMTEC applications; namely, long-life, high-power electrodes.

B. Technology Status

Work on the LMTEC concept to date has been focused on the development of a long-life, high-power, porous electrode. The best state-of-the-art electrodes are composed of either magnetron

sputter-deposited molybdenum 1-3 micrometers thick or a bi-conductor cermet composed of a mixture of molybdenum and BASE powders. In the case of the thin-film molybdenum electrode, power densities are initially high (near theoretical), but the power output decays by a factor of 3-5 in the first 1000 hours of operation (7,12). Power output usually remains stable thereafter. Power densities for the cermet electrode, although not as high initially, have been observed to remain stable for up to approximately 10,000 hours (13). Present research has been directed toward maintaining the initial high output of molybdenum thin-film electrodes, where recent results have for the first time led to the elucidation of the mechanisms that determine electrode performance. Work is now proceeding to identify means to stabilize electrode performance based on those results.

Testing self-contained recirculating devices has generally been limited to single-cell units operating at <100 W power levels. One multi-cell series-connected device has been operated for a brief period at 111 W (13).

C. Technical Issues

The laboratory experiments and applications studies conducted to date have shown that the LMTEC concept possesses great promise. However, it is still at an early stage of development relative to more mature energy conversion devices. Thus, a substantial technology development effort will be required before prototype solar thermal units can be field tested. Previous analyses on LMTEC have led to the conclusion that to bring the LMTEC to a state of technical maturity for solar applications, several key questions must be answered. They are

1. How should the LMTEC be integrated with a solar receiver? Is

direct or indirect heating (e.g., through heat pipes) superior for heating the hot metal reservoir?

2. Is a distributed receiver or central receiver technology better suited for adaptation of the LMTEC?

3. Is there any bottoming cycle that can be coupled with the LMTEC in a solar thermal system to improve the overall efficiency?

4. What methods are available for the reduction of parasitic losses?

a. What materials and surface treatments will ensure a smooth reflective surface for the cool condenser area?

b. Can the electrochemically active electrode area be increased relative to the radiative area of the electrode?

c. Can a radiation shield be designed that will not greatly impede the flow of metal vapor to the condenser surface?

5. What are the effects of the thermal, electrical, and mechanical transients on the durability of the device? Will special start-up or shut-down procedures be required?

6. What are the power conditioning needs? How will the need for redundancy and the high output voltage affect the choice of individual cell size in a series-connected LMTEC?

7. What are the projected manufacturing costs for the LMTEC as a function of power output and specific application? What are the serviceability and maintainability considerations?

8. What composition and morphology are required to produce a long-life electrode with close to theoretical output power? What is the optimum technique for making reliable, low-resistance connections between the output current bus and the porous electrode?

Items 1 - 6 have been addressed and continue to be addressed in

designing the LMTEC. Item 7 remains to be addressed when more definite ideas on materials and configurations required are available. Item 8 has been approached, and a decision has been made to proceed with the analysis and design of LMTEC for solar thermal applications, assuming the current electrode technology is what is actually available. Nevertheless, because improvements in electrode technology stand to make significant improvements in the projections for the LMTEC, research to improve the lifetime of high power density electrodes is essential. The research and results reported in this document were directed toward meeting this goal.

II. PROGRAM OBJECTIVES AND CONTENT

The objective of this program was to experimentally investigate new electrode materials and configurations, and to identify improved durability, high-power electrodes for possible solar thermal application. Pursuant to Sandia Purchase Order 64- 9358, the specific technical tasks as specified in the statement of work were

1. Design and fabricate a recirculating test cell for the purpose of conducting long-term testing and evaluation of various electrode materials, configurations, and deposition techniques. The design of the test cell should be flexible enough to address more than one problem issue associated with electrode research. It is intended that this test cell be made available to conduct experiments affecting issues that may be raised by Sandia at a later time in the contract.

2. Perform research on various refractory metal, refractory metal alloy, and metal oxide electrode materials deposited by various sputtering or evaporation techniques that can be used in a sodium LMTEC with the goal of maximizing long-term power density. Research on the molybdenum electrode should be pursued to ascertain the mechanism involving Na/Mo bronzes on the surface of the electrode pores and to establish a possible method for stabilizing these bronzes. Any promising electrode composition identified during the course of this contract will be pursued by the contractor at the discretion of Sandia.

3. Characterize the electrochemical behavior of the various electrode materials with an emphasis on those appearing more promising for short-term application to LMTEC. This characterization should address the transport properties of sodium at the porous electrode-beta"-alumina

interface using various measurement techniques including but not limited to voltage/current and current-interrupt techniques. The cell voltage versus current density measurements should be made as a function of temperature and time. The time duration for these measurements should be a minimum of 100 to 1000 hours depending on the behavior of the electrode. Measurements for longer times may be specified at a later date as the need may warrant. A measure of the electrical sheet resistance in the plane of the electrode shall be made.

The fast current-interrupt measurements should be performed after establishing the steady-state current density for the electrode by the use of a suitable fast transistor switch while the cell voltage is recorded with a storage oscilloscope. The purpose of these measurements is to determine the pressure drop across the electrode. The pressure drop should be determined as a function of time and electrode degradation. The rate of sodium desorption from the electrode surface after current interruption should be followed by a suitable technique such as residual gas analysis (RGA).

4. Perform suitable physical and chemical analytical measurements to establish the chemical, structural, and morphological characteristics of the electrodes tested, including but not limited to:

-crystallinity by x-ray diffraction (XRD),

-changes in surface morphology and pore size by hot-stage Scanning Electron Microscopy (SEM),

-chemical composition by energy dispersive spectrometry and/or ion microprobe,

-chemical composition and oxidation states of electrode degradation products by a suitable <u>in situ</u> spectroscopic technique.

These measurements must be performed before and after high- temperature cycling and sodium electrolysis. In the case in which a transient species may be involved, in situ measurements may be necessary during the high-temperature operation of the cell. Any corrosion reactions taking place at the interface between the beta"-alumina and the electrode material must be characterized.

5. Various cell electrode configurations should be tested to determine if differences in the coefficients of thermal expansion for the beta"-alumina and the Mo electrode give rise to electrode separation as a result of temperature cycling. This will require that Mo or other suitable electrode be deposited on the inside of a beta"-alumina tube of approximately one-inch internal diameter. Several deposition techniques must be tried and tested to establish the optimum method in terms of performance and practibility

6. In the event that some periodic electrode treatment technique becomes necessary, it should be developed with the solar end-use as the intended application.

The following sections in this report describe work performed in attempting to fulfill the tasks listed previously. The experimental techniques and the electrochemical, chemical, and physical measurements used in connection with items 2, 3, and 4 of the work statement are described in Section III. The results of research on three different electrode systems are described in Sections IV, V, and VI, where each section addresses items 2, 3, and 4 of the work statement for each electrode concept. Two of the electrode systems (Sections V and VI) show considerable potential for meeting program objectives and these results constitute major progress in electrode development.

Section VII describes alternative electrode deposition concepts that

could be utilized to deposit electrodes inside of BASE tubes in connection with item 5 of the work statement. Since the techniques studied could not be developed satisfactorily within the resources of this task, no subsequent testing of electrodes deposited inside BASE tubes was attempted. However, additional work could still lead to a high-quality deposition technique as an alternative to magnetron sputtering. Some of these alternative techniques were concurrently addressed by Sandia in attempting to deposit a porous electrode inside a BASE tube.

Section VIII contains the concept design for a recirculating test cell in connection with item 1 of the work statement. Assembly and testing of this device were not carried out due to delays in obtaining preliminary data necessary for its assembly. Emphasis was thus placed on the Electrode Test Cell studies described in Sections IV - VII. With regard to item 6, we have concluded that periodic electrode treatment is not a desirable approach to long life, high power operation (see Section IV).

III. EXPERIMENTAL TECHNIQUES AND ELECTRODE TEST CELL DESCRIPTION

LMTEC electrode research has been carried out in the demountable, electrode test cell (ETC). A schematic diagram of the ETC is given in Figure 2 and more detailed diagrams follow. Figure 3 shows the BASE tube plumbed to the top 2-3/4" flange via O-ring seals, with heater well, thermocouple well, voltage probe, and stainless steel mesh wick visible in the interior of the BASE tube. Figure 4 shows the external leads to two electrodes on the tube as well as the heat shield and its support. Figure 5 shows an external view of the demountable test cell vacuum chamber, and Figure 6 shows the pumping system used with both the demountable ETC and the recirculating test cell.

In practice, the LMTEC vacuum chamber is evacuated first with the mechanical pump, then the turbomolecular pump is used while degassing the tube and for general use. Typical system pressures achievable with this combination of pumps are in the range of 1×10^{-5}. When lower pressures are desired, the ion pump can be used, provided no small argon leaks are present through the BASE tube or at the O-ring area.

In setting up the ETC, the BASE tube containing 10 - 17 grams of sodium is loaded under argon and then connected to a supply of high-purity argon, which is maintained at a pressure of slightly greater than 1 atmosphere over the liquid sodium during the experiment. This prevents rapid heat exchange between the hot sodium reservoir and the top of the tube via sodium evaporation and condensation. Next, a thermocouple well containing a type-K shielded thermocouple is spot-welded to the heater well. This welded assembly along with a voltage probe is wrapped in stainless steel mesh to help wick the sodium within the BASE tube. The thermocouple well and heater well are shown in Figure 2, and the relative

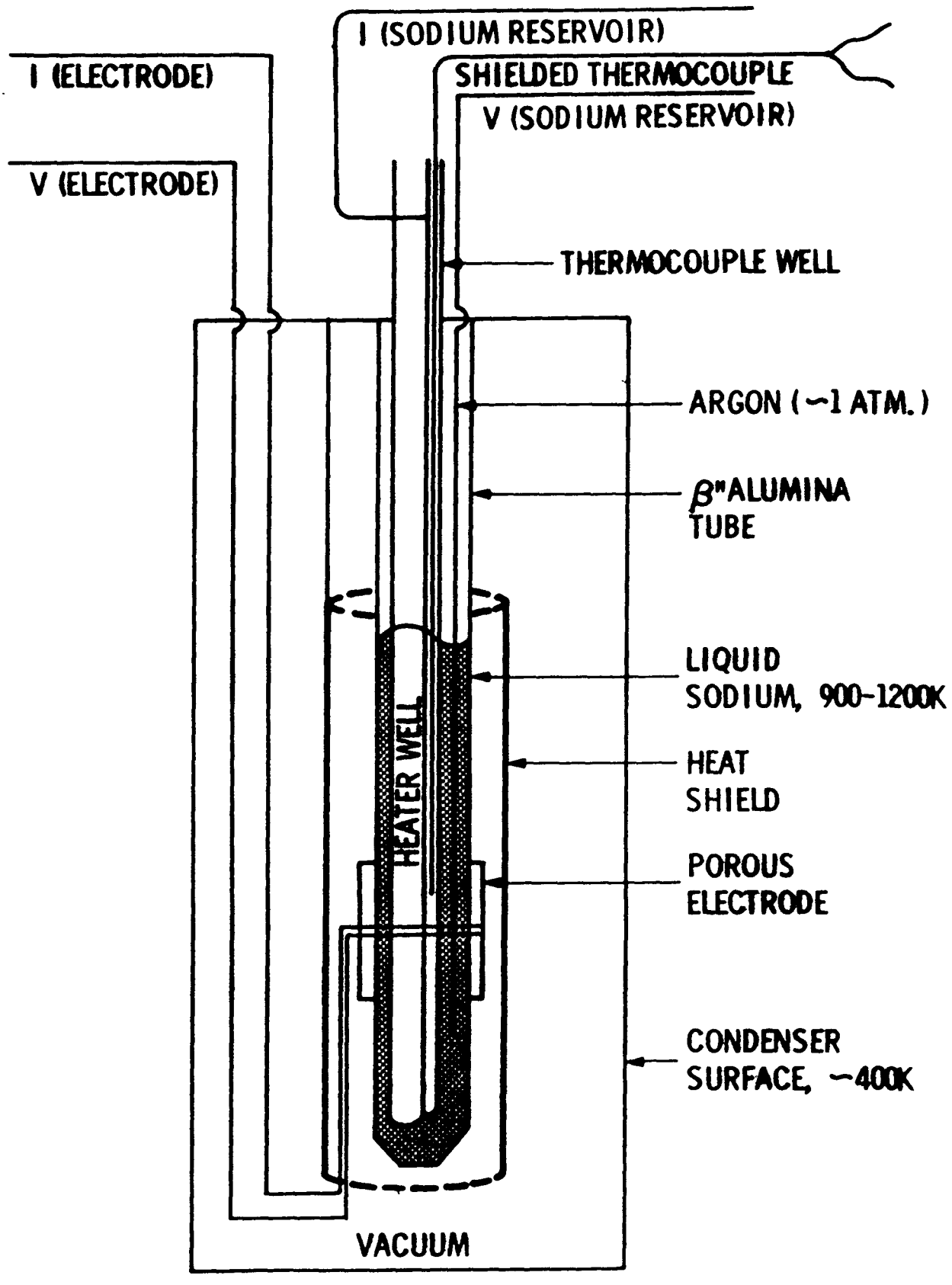

Figure 2. ETC Schematic Diagram.

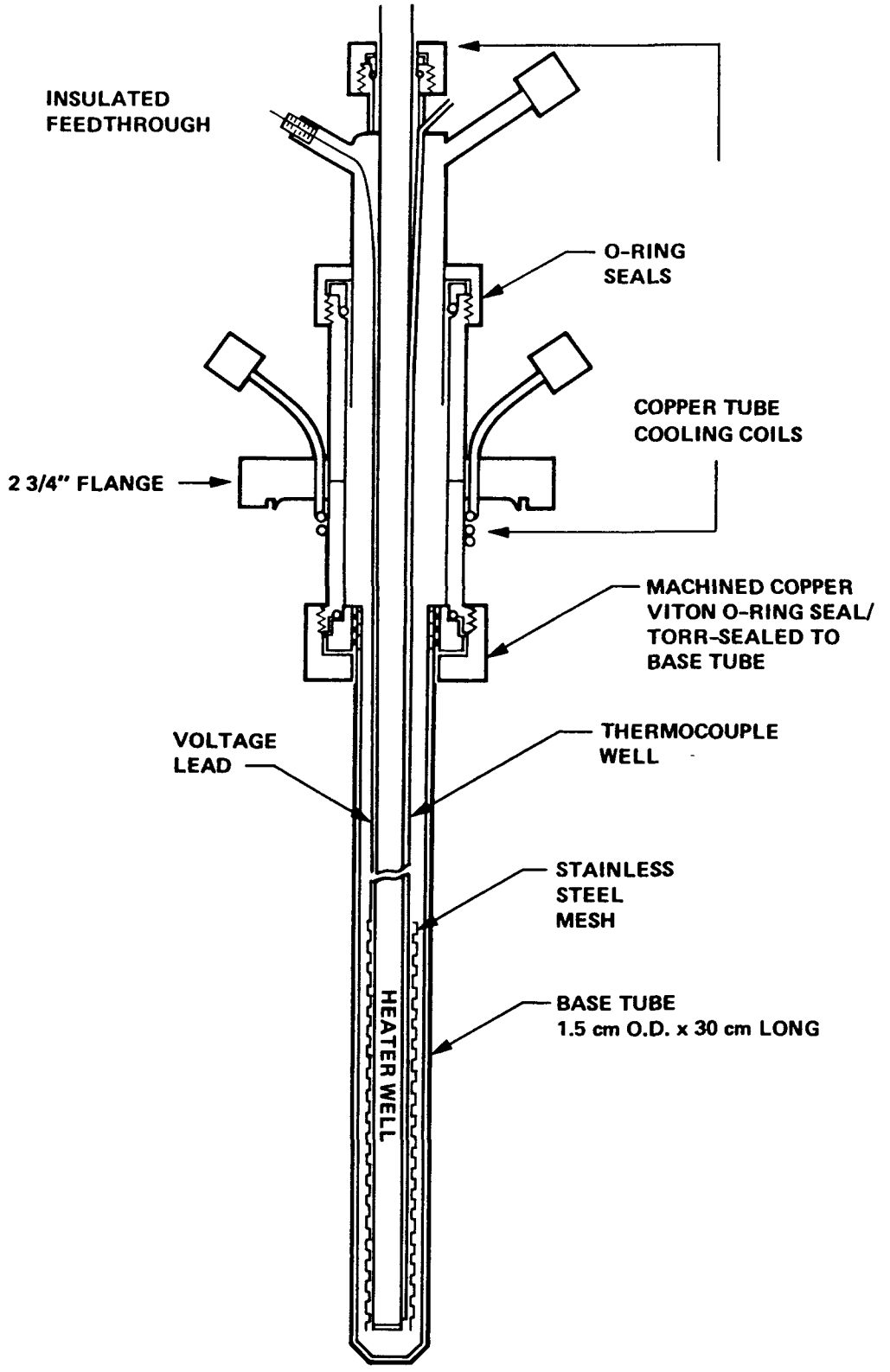

Figure 3: BASE Tube - Heater Well - Thermocouple Well - Central 2 3/4" Flange Assembly

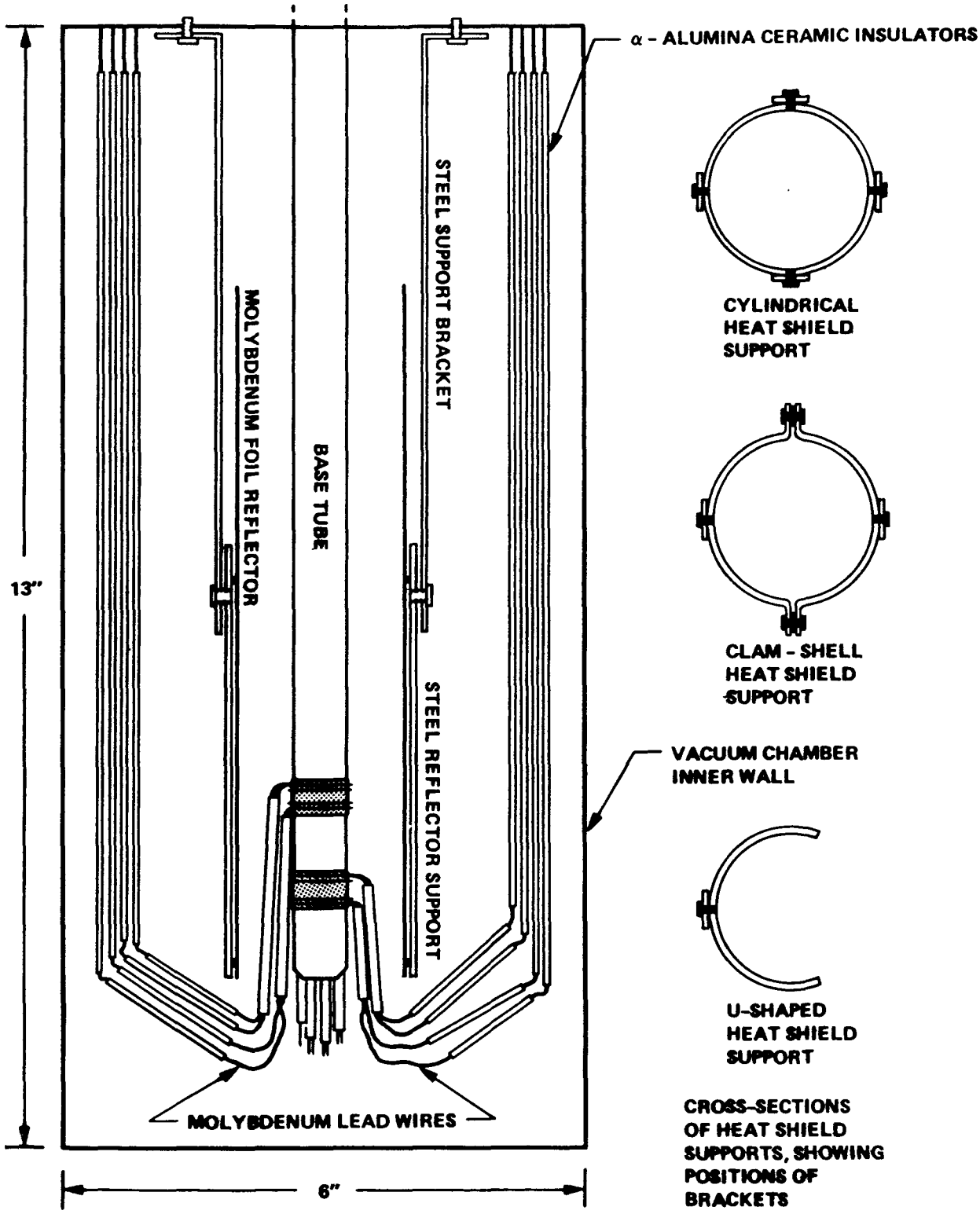

Figure 4: Internal Geometry of Demountable Electrode Test Cell Vacuum Chamber, Showing BASE Tube, Electrodes, Electrical Leads and Heat Shield

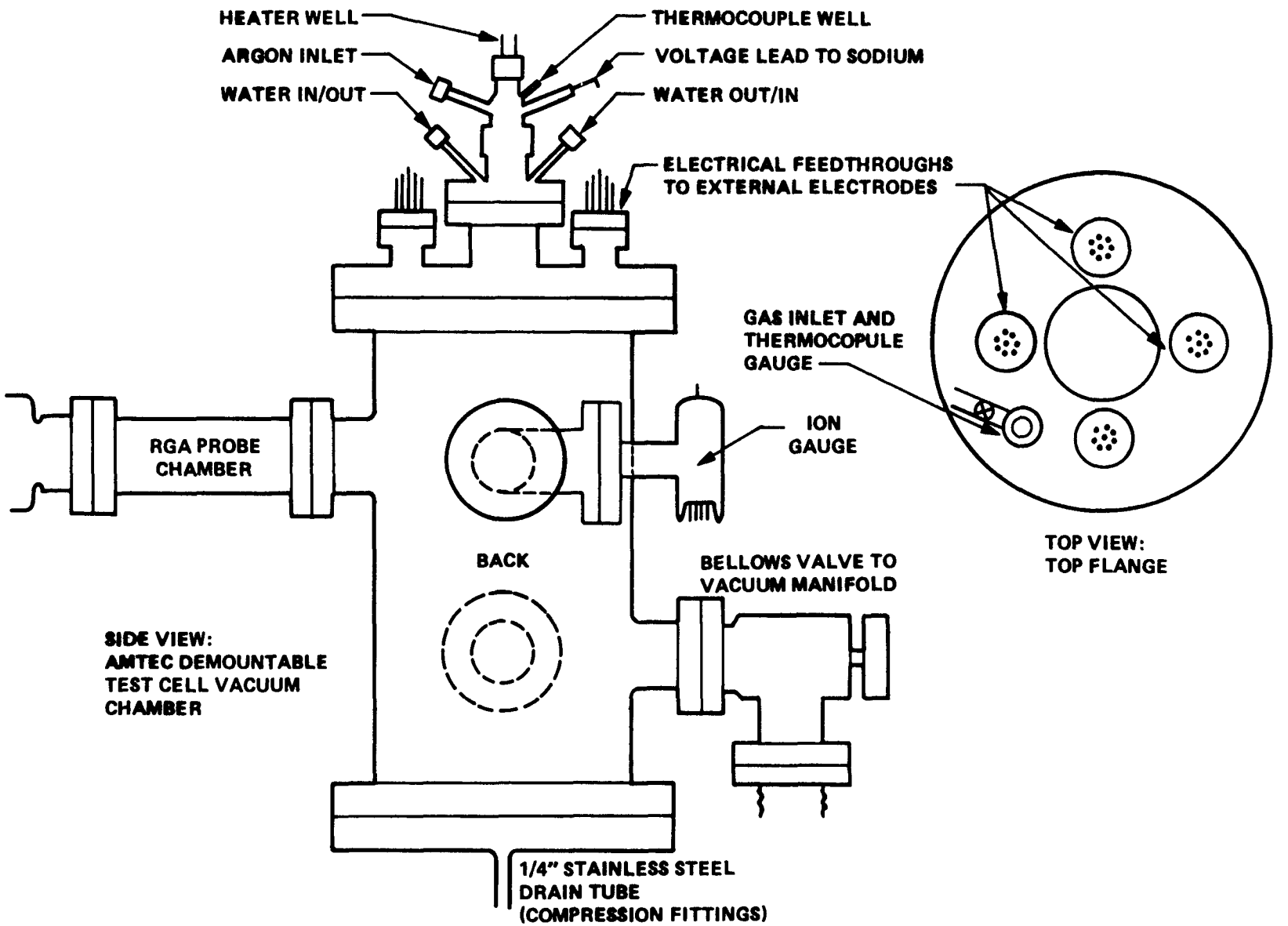

Figure 5: External View of Demountable Test Cell Chamber

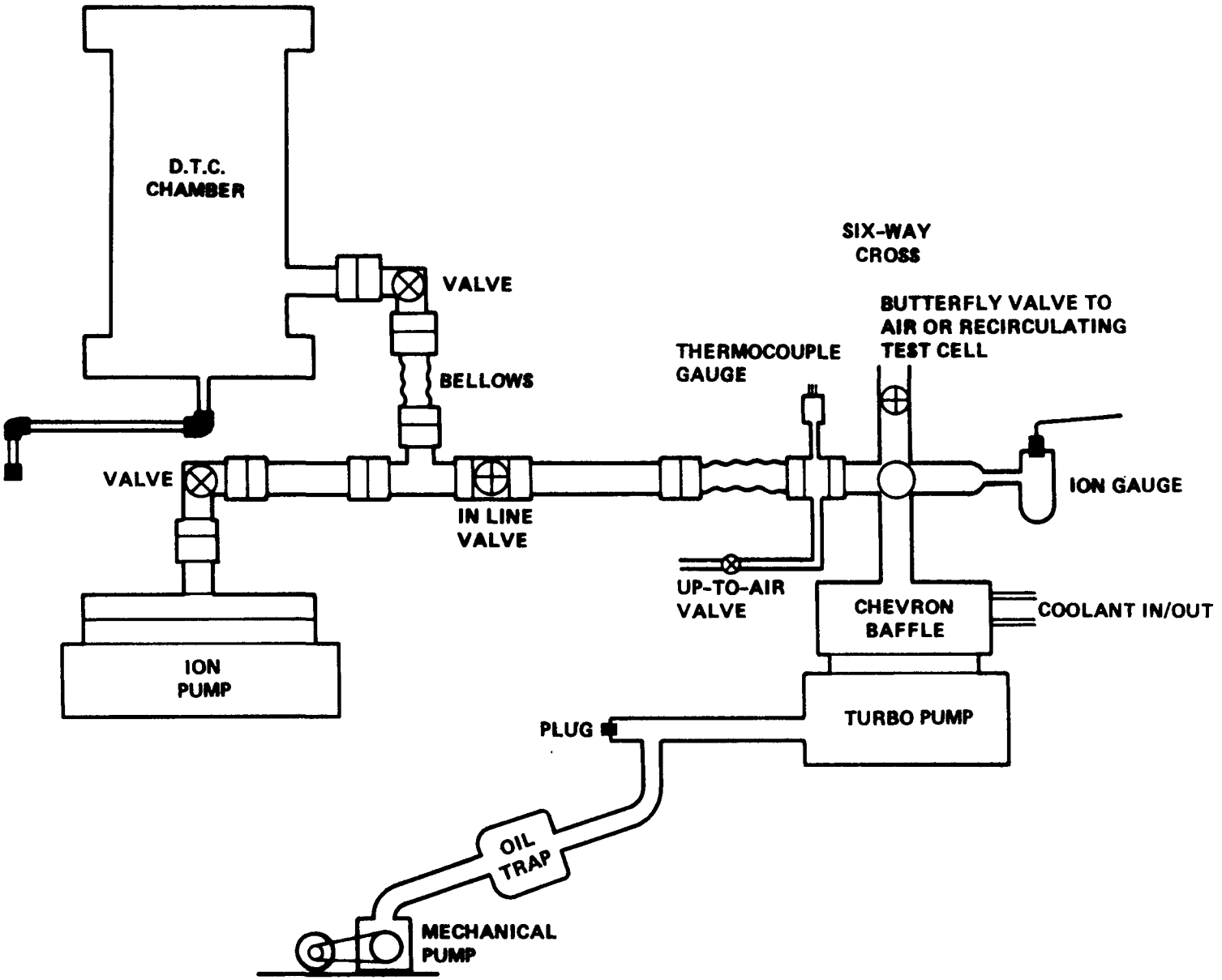

Figure 6: Demountable Electrode Test Cell Pumping System

position of the stainless steel mesh and the voltage probe is seen in Figure 3. The mesh-wrapped assembly, mounted to its 2-3/4" flange with associated plumbing and feedthroughs, is then carefully lowered into the BASE tube containing the molten sodium and mated to it via an O-ring seal to a copper collar bonded to the BASE tube with Torr-Seal (Varian). This Torr-Sealed area is illustrated in Figure 3. Since the O-ring seal is water-cooled and only the lower portion (14 - 18 cm) of the BASE tube is kept at typical LMTEC operating temperatures (1000 - 1200 K) by the heater and heat shield, the top of the tube remains relatively cool (473 K) and generally little thermal degradation of the O-ring or Torr-Seal was observed. Composition of the LMTEC cell atmosphere in the sodium vapor region was monitored for leaks and outgassing products with an Anavac residual gas analyzer.

The vertical temperature gradient along the tube is measured at a nominal temperature (1000 - 1100 K) which is near the maximum cell operating temperature and in most cases at a lower temperature (500 - 700 K). All subsequently measured temperatures were taken at one location and temperatures along the tube were determined by linear interpolation and extrapolation from the observed temperature gradients. The heat shield used consisted of a cylindrical Mo foil, which surrounded the hot zone of the BASE tube at a distance of 1.0 - 1.5 cm.

Current-voltage characteristics of the LMTEC cell were determined using a four-probe configuration with separate current and voltage leads to both the sodium reservoir and the external porous electrodes. The heater well was used as the current lead from the sodium and it was connected to the external vacuum chamber at ground. The sodium reservoir voltage lead was insulated with alumina tubing above the liquid sodium and exited ν a an insulated feedthrough. The insulated voltage lead was used

to determine the true cell potential when large currents, up to 10 A, would result in a significant i-R drop along the current lead. Solid nickel alloy or Mo rod feedthroughs were connected to 1.2-mm diameter Mo wire current leads and 0.5-mm diameter Mo wire voltage leads to the external electrodes.

The arrangement for conducting current at the electrodes consisted of one or more 0.5-mm Mo wires snugly encircling the tube at each elecrode and secured by twisting the ends together. In addition the wires were brazed to the Mo electrode by the use of a ball-milled mixture of Nicrobraze LM (a nickel-base brazing alloy available from Wall Colmonoy Corp., Detroit, MI) and Mo powder in a ratio of 62/38. The braze mixture was made into a slurry with Nicrobraze cement and acetone and painted onto the Mo electrode under the Mo tie wires. The whole assembly was then placed on a quartz tube and heated inside a tube furnace to approximately 1325 K for 5 - 10 minutes under one atmosphere of purified, dried argon gas.

In a separate study, this braze procedure was found to be the optimum for Mo wire on thin-film Mo electrodes. The ability to obtain repeated, good physical and electrical contacts made this an important development in the study of Mo electrodes. The leads from the feedthroughs were crimp-connected to leads from these contacts near the bottom of the tube (2 - 4 cm from the electrodes) or near the top of the tube above the heat shield.

Porous Mo electrodes were deposited by magnetron sputtering from a cylindrical Mo target under a pressure of 5 millitorr argon onto a rotating, masked BASE tube. The BASE tubes were manufactured by Ceramatec, Inc., Salt Lake City, UT, and had a nominal 15-mm outside diameter, 300-mm-long, 1.2-mm wall thickness, and were made from lithia

stabilized sodium beta"- alumina. The sputtering system was operated at a typical pressure of 2.5×10^{-6} Torr with no bias or heating of the substrate and a typical deposition rate of 14 angstroms/second. BASE tubes were kept under vacuum or in an argon filled glove box at all times before the experiments, except during transfers and for wiring of the electrode contacts to the feedthroughs. BASE tubes were evacuated for 12 - 16 hours in the sputtering system prior to porous electrode deposition.

The in situ oxidation studies were performed by admitting air or oxygen into the vacuum chamber and the exterior of the BASE tube under controlled temperature, pressure, and exposure time. Oxygen exposures were carried out at elevated temperature and low pressure for 10 minutes. Air oxidation was performed by opening the vacuum chamber to the atmosphere for 20 minutes at room temperature.

In several experiments a slurry of Na_2MoO_2 in propanol was painted onto the porous Mo electrodes prior to pumping down the system. Some Mo electrodes were exposed to low-pressure air (5 - 10 mTorr) in the LMTEC chamber during heating to approximately 650 K.

The test conditions, including operating temperature and cell voltages, were limited for some electrodes. These two parameters detemine current densities and, hence, sodium activities in the porous electrodes. It has been shown in previous work (2) that the effective sodium pressure at the exterior surface of the electrode, $P_{EFF.}$, in Torr, can be determined from the current density, j, in A/cm^2, and the temperature, in degrees K:

$$P_{EFF.} = 8.55 \times 10^{-4} T^{1/2} j \quad . \qquad [1]$$

Therefore, controlling the operating temperature and cell voltages allows estimation of the position of equilibria associated with some of the chemical reactions occurring in the electrode. All electrodes were

left at open circuit when measurements were not being performed.

LMTEC cell measurements at currents greater than 0.1 amp were made using a potentiometer-controlled power FET, in series with a current supply, in the four-probe configuration. Measurements at less than 0.1 amp were carried out with an EG&G Princeton Applied model 175 universal programmer, Model 173 potentiostat, and a Model 176 current follower in a two-probe configuration with the sodium reservoir (at ground) as the working electrode and the external electrode as counter electrode and reference. The ac impedance spectra were also obtained in the two-electrode configuration over the frequency range of 0.01 Hz to 20 kHz using the potentiostat in conjunction with a Model 276 interface, a 5206 lock-in amplifier, and an Apple 2e computer. All the electrochemical data presented in the data involved the sodium reservoir as the reference. This is deemed reasonable since the [Na] = 1.0 in the sodium reservoir under one atmosphere of argon and the activity of Na^+ in BASE is close to unity and is a constant due to the virtual non-polarizability and large area of the sodium/BASE interface.

Power densities, impedance characteristics, and morphological and chemical changes were studied in parallel for electrodes that varied by composition, lead configuration, chemical treatment, or other parameters. Morphological studies of electrodes were carried out by scanning electron microscopy (SEM) with as-deposited porous Mo films, similar films following heat treatment in argon (brazing), and similar films following LMTEC cell operation for periods up to 220 hours mostly at open circuit. Both the exterior surface and the fracture cross-section of electrodes were studied by SEM and energy dispersive spectroscopy (EDS) following the experiments. In addition, small rectangular BASE chips were used to determine the as-deposited morphology of the films. In general, small

BASE chips were wired to the tubes between electrode strips during electrode deposition to characterize the as-deposited Mo electrode thickness and porosity. Since a brazing step was often employed, a few chips were left on the tube in order to determine the effect of this high-temperature processing on film morphology.

The x-ray diffraction studies were carried out using a locally designed, constructed, and calibrated Guinier camera with a focusing quartz crystal monochromator and CuK-alpha radiation. The camera was operated in vacuum to minimize the background due to scattering as well as to protect the air-sensitive samples.

Sheet resistance measurements were performed on electrodes to determine the relative importance of this parameter compared with the ionic resistivity of the BASE and the electrode impedance to sodium flow. Four-probe and two- or three-probe resistance measurements were carried out before, during, and after cell operation to characterize both the sheet and contact electronic resistances.

Multiple probes are also useful for measuring the voltage profile across the electrodes in order to determine the spatial dependence of electrode utilization on sheet resistance. In practice, the current was scanned at one contact while measuring the voltage at each of a series of separate contacts.

In order to simulate sodium activity levels at LMTEC operational conditions with large samples and components, experiments were carried out separately in evacuated stainless steel tubes sealed on the bottom and valved at the top. The samples were placed at a known position in the tube, which contained 1 - 2 grams of sodium. The temperature of the entire system was controlled with a furnace and heating tapes. When very low s dium pressure was to be used, evacuation continued throughout the

experiment. Components were frequently pre-screened in this manner prior to full LMTEC experiments.

Further details of electrode and sample preparation are given in the following sections of this report.

IV. STUDIES OF THE EFFECTS OF SODIUM MOLYBDATE ON MOLYBDENUM LMTEC ELECTRODES

A. Introduction

Previous work was concerned with the chemistry of Mo electrodes in the LMTEC environment, i.e., temperatures between 1000 and 1200 K, low pressures, and greatly varying Na activity. It was determined that molybdenum oxides were present initially and that Na-Mo-O compounds played a great role in the electrode operation. After the Mo electrodes are deposited by sputtering, exposure to air creates molybdenum oxides, which in the presence of Na form various Na-Mo-O compounds, the exact stoichiometry of which depends on temperature and sodium activity. The compound Na_2MoO_4 in particular has been suggested to be important since it is a good ionic conductor, and at the LMTEC operating temperatures it is a liquid that would tend to be more evenly distributed in the pores of the Mo electrode. Another compound, $Na_2Mo_3O_6$, may also be an ionic conductor. It is known to be an electronic conductor that is expected to be of importance. These two compounds can be interconverted depending on the temperature and sodium activity:

$$2\ Na + 2\ Na_2Mo_3O_6 \rightleftharpoons 3\ Na_2MoO_4 + 3\ Mo\ . \qquad [2]$$

This interconversion is important because Na_2MoO_4 has a significant vapor pressure at the LMTEC operating temperature and would evaporate from the electrode. In this section, further studies to determine the role of Na-Mo-O compounds on the Mo electrodes in the LMTEC device will be presented.

Direct application of sodium molybdate to sputtered Mo electrodes was carried out in two LMTEC experiments. In all cases, these treated electrodes exhibited unique behavior, including higher initial power

densities, slower initial degradation than in the case of untreated electrodes with much smaller quantities of fortuitously formed oxides, higher sheet resistances where measured, and other differences determined by impedance measurements and morphology studies. Regeneration under cell operation has also been observed for partially degraded electrodes, although at later stages of degradation, regeneration by sodium exposure (cell operation) becomes impossible. A fairly detailed picture of the chemical and morphological changes that occur in the life of sodium molybdate- treated Mo electrodes may be inferred from these results. At moderately high LMTEC operating temperatures (1100 - 1200 K) these changes include fairly rapid evaporation of sodium molybdate and reaction of sodium molybdate with Mo, slow loss of low concentrations of sodium molybdate in equilibrium with $Na_2Mo_3O_6$, electrochemical sintering of Mo due to continual interconversion of Na_2MoO_4 and $Na_2Mo_3O_6$, and sintering of Mo after loss of all Na-Mo-O phases.

B. Experimental

Sputtered Mo electrodes were prepared as described elsewhere (Setion III). A variety of current collector and lead configurations was employed with cylindrical electrodes: two Mo contact loops; four Mo contact loops; and handmade Mo grids. Contact loops were brazed on for two and four-loop configurations and sometimes with the handmade Mo grids. Sodium molybdate was painted on as a slurry in propanol at estimated amounts of from 2 to 5 mg/cm^2. A variety of *in situ* electrical and electrochemical measurements was made over a range of temperatures, as well as at high temperature during the life of the experiment. Post mortem characterization included scanning electron microscopy and x-ray diffraction studies when permitted by the nature of

the experiment termination.

C. Results and Discussion

Figures 7 and 8 show the dependence of maximum power with time for two experiments, each of which involved both treated and untreated electrodes of similar thicknesses, initial morphology, and lead/contact configuration. Electrodes were kept at open-circuit between measurements. The effects of regeneration following high current density operation experiments (repeated i- V curves and repeated current interrupt experiments) are indicated in Figure 7. The data clearly indicate an extended period of high power density performance at high temperature, compared with untreated electrodes which rapidly reached a lower power performance level

Sheet resistance data for initial warm-up of electrodes treated with sodium molybdate are compared in Figure 9 with sheet resistances of untreated electrodes. Increased sheet resistance results from corrosion of highly conductive Mo by Na_2MoO_4 to form the less conductive $Na_2Mo_3O_6$, a reaction that begins to proceed at a high rate between 900 and 1000 K. Thus, sheet resistances for the treated electrodes are higher than for the untreated electrodes above 900 K (Figure 9).

The presence of an ionic conductor in the porous electrode should change the nature of the transport processes significantly. Charge transfer resistances should be reduced for two reasons: (1) sodium activity is reduced in the electrode due to reduced sodium back pressure, and (2) the charge transfer process itself should be made more efficient due to an increase in the effective reaction area. Table I contains compilations of data for Mo electrodes of total internal resistance (from curren. interrupt experiments), ionic resistance (from ac impedance

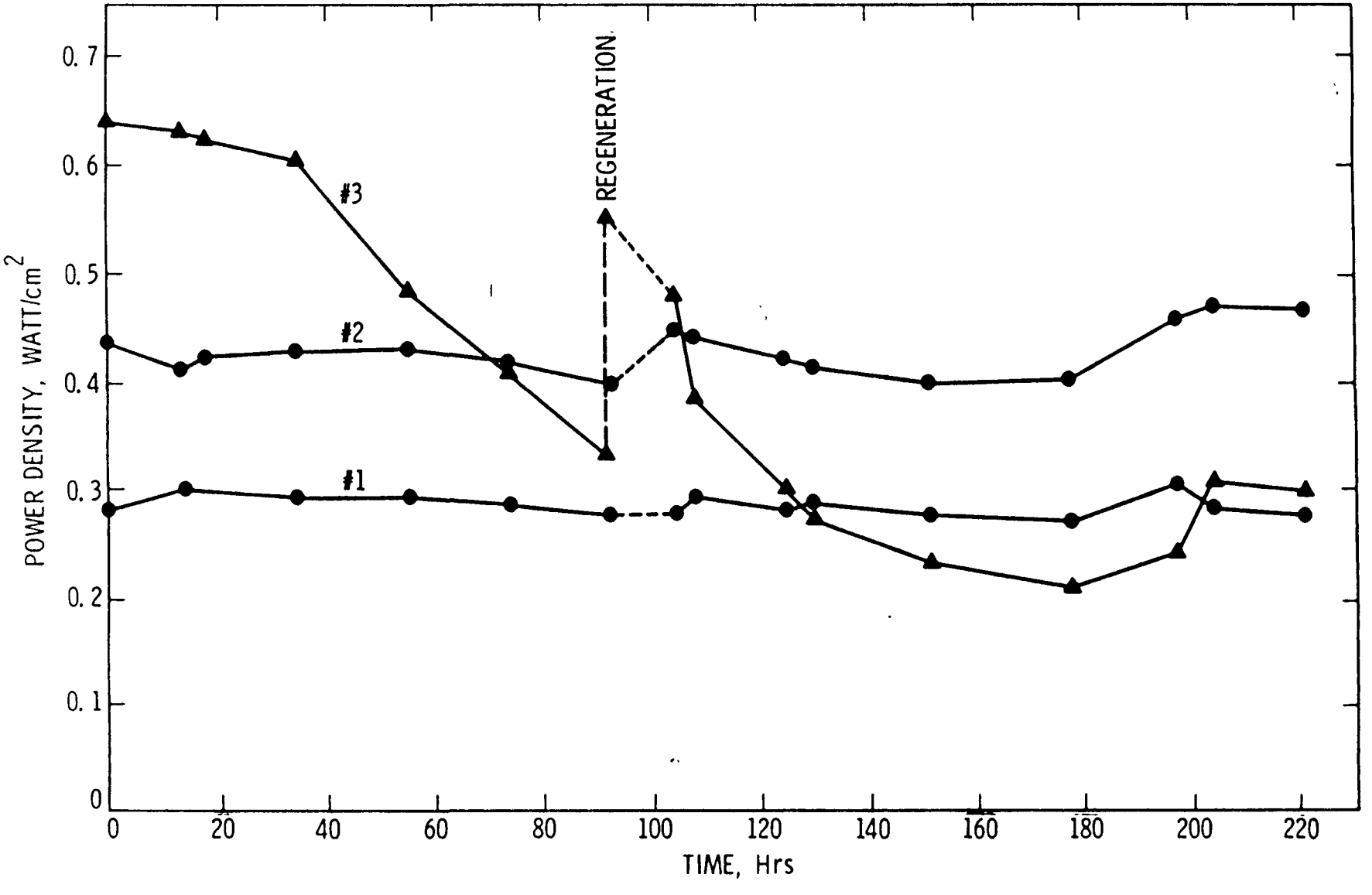

Figure 7: Power densities vs. time for porous molybdenum electrodes. #1: 0.45 μm Mo; #2: 2.5 μm Mo; #3: 2.5 μm Mo treated with Na_2MoO_4, showing regeneration at 90 hours. All electrodes have T_2 ≈ 1100K, brazed loop contacts.

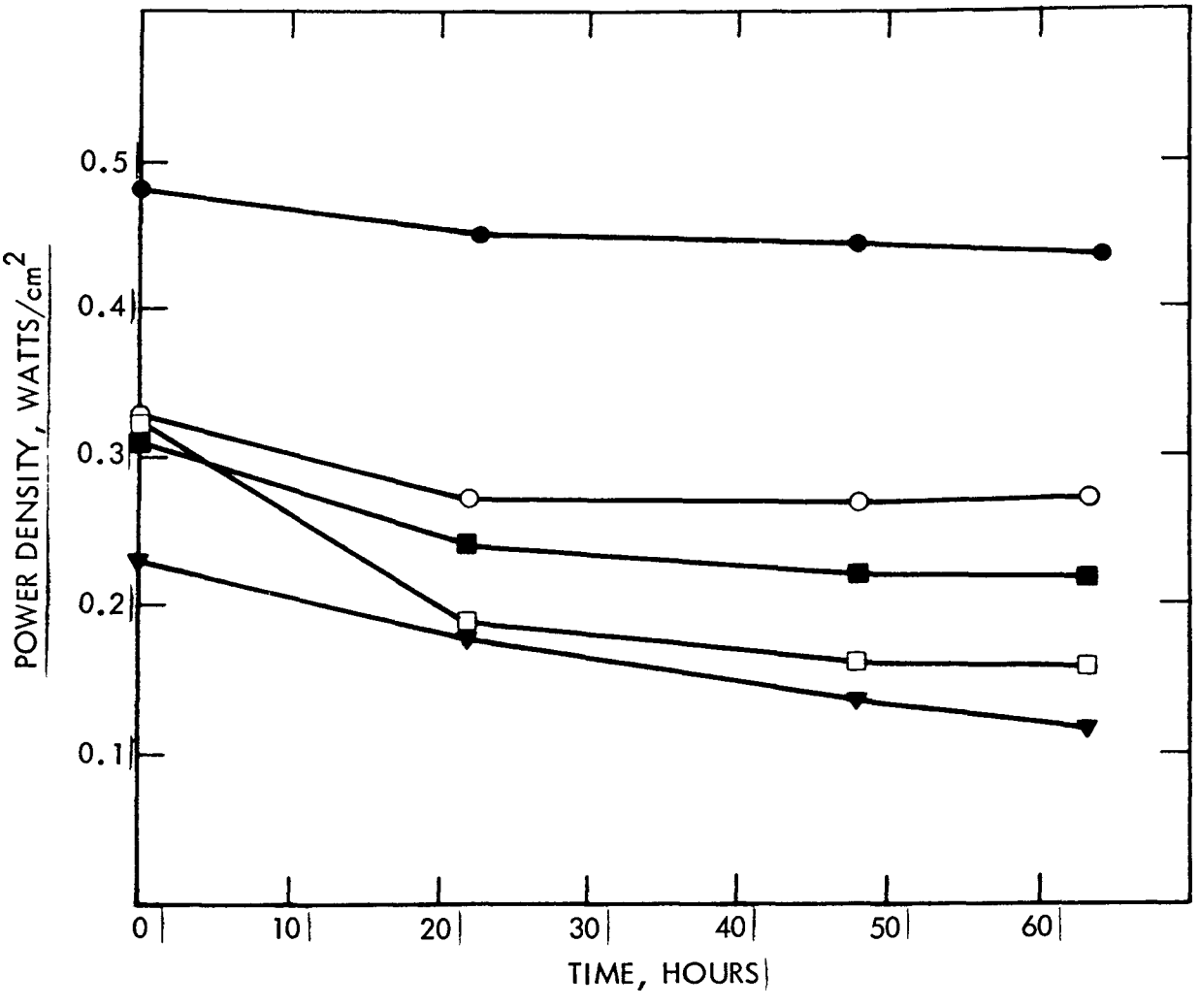

Figure 8: Maximum Power Densities vs. Time for $Na_2 MoO_4$-Treated and Untreated Porous Molybdenum Film (1.4 Microns Thick) Electrodes

●: Na_2MoO_4 Treated, Mo Wire Grid Contact, 1078 K

○: Na_2MoO_4 Treated, Single Mo Loop Contact, 1096 K

□: Untreated, Single Mo Loop Contact, 1108 K

■: Untreated, Mo Wire Grid Contact, 1083 K

▼: Untreated, Mo Wire Grid Contact, 1074 K

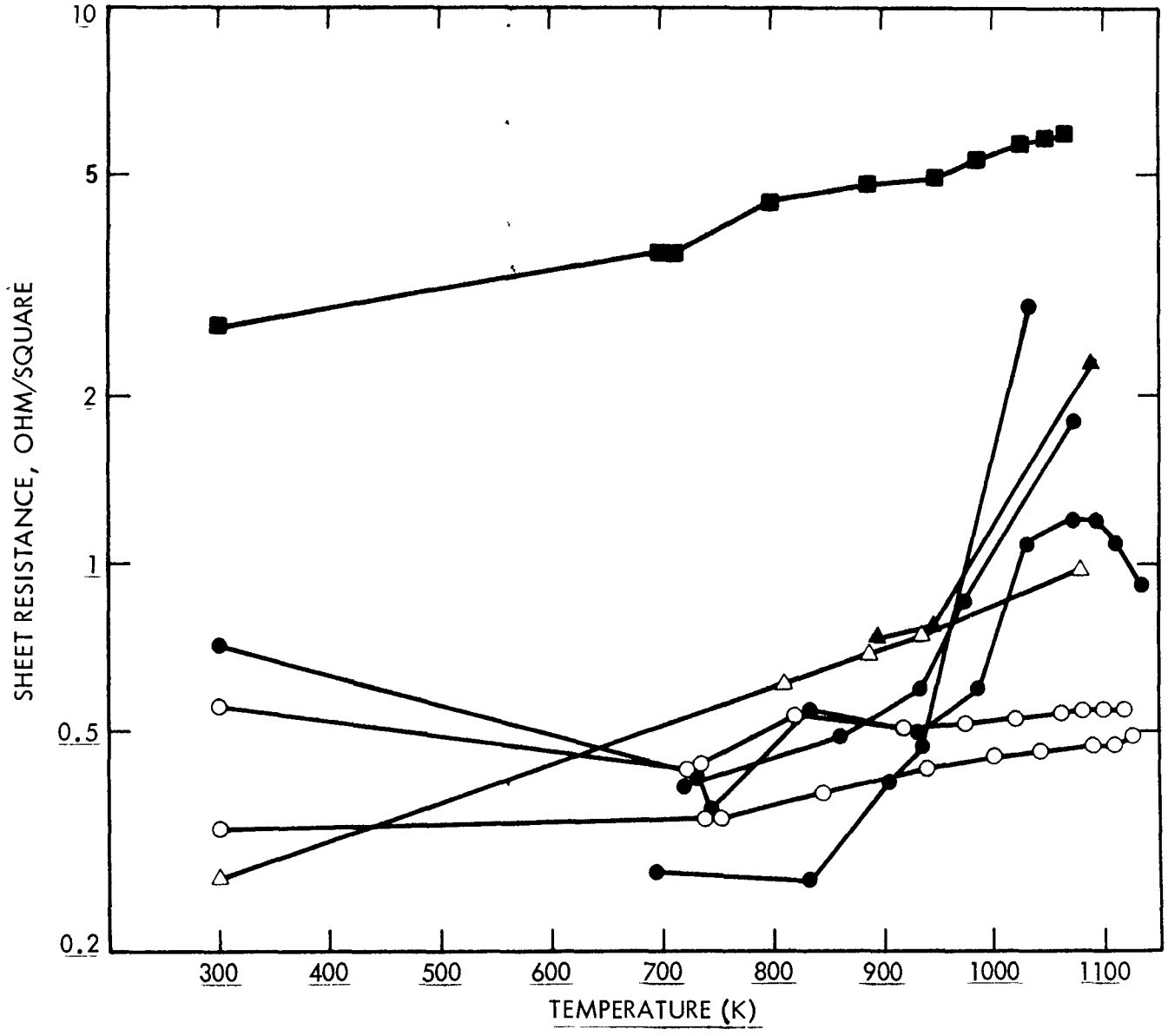

Figure 9: Sheet Resistances of Porous Molybdenum Electrodes Treated with Sodium Molybdate (● 2.5 Micron Film, ▲ 1.4 Micron Film) and Not Treated (○ 2.5 Micron Film, △ 1.4 Micron Film, ■ 0.45 Micron Film).

Table I

Typical Internal Resistances

in Molybdenum Electrodes

	Total Internal Resistance (From Current Interrupt) Ohm-cm^2	Ionic Resistance (From A.C. Impedance or Calc for BASE)	Electrode Electronic Sheet Resistance (2 Probe) Ohm/square
Untreated 0.45 μm	0.56	0.20 calc	5.90
Untreated 2.5 μm	0.25	0.20 calc	0.52
Fresh Na_2MoO_4 Treated, 2.5 μm	0.42	0.47 grid 0.74 loop	~2.0
Degraded After Na_2MoO_4 Treatment, 2.5 μm	0.34	0.20 calc	0.54

experiments), and sheet resistance. Sheet resistances can be seen to have relatively little effect on the series electronic resistances due to reduction in electrode area utilization for more resistive electrodes.

Since the ionic resistance of the BASE is somewhat variable, depending on the history and exposure to the atmosphere, a comparison of the treated and untreated electrode data from the same tube is most useful. Fresh BASE tubes with minimal exposure to air exhibit contributions to the ionic resistance of about 0.2 ohm-cm^2 at typical LMTEC operating temperatures. Figures 10 and 11 show a collection of ac impedance data for Mo and Na_2MoO_4 - treated Mo. The single semicircular shape observed in Figure 10 for the untreated electrode is potential dependent and can, therefore, be attributed to the interfacial capacitance and charge transfer resistance at the BASE-porous electrode interface. Figures 11a & b show ac impedance data consisting of a potential-independent, transient, high-frequency semicircle due to the ionic conductor (Na_2MoO_4) and a potential-dependent, low -frequency semicircle due to the Na_2MoO_4-Mo interface.

Due to the presence of Na_2MoO_4, the total resistance to ionic transport should increase since sodium ions migrate through both the BASE and the electrode. The increase will be slight when pores are filled with the molten salt, but after reaction with the metal matrix, only small quantities of molten metal will be present, and a higher total inoic resistance will be observed as the area of the ionic conductor decreases. This may be detected as a larger contribution to the i-R drop observed in current interrupt experiments as well as a larger high-frequency loop, which disappears as the electrode degrades (Na_2MoO_4 evaporates), in the ac impedance spectra. However, the measured ionic resistance shown in Table I is not identical to the ionic resistance that contributes to the

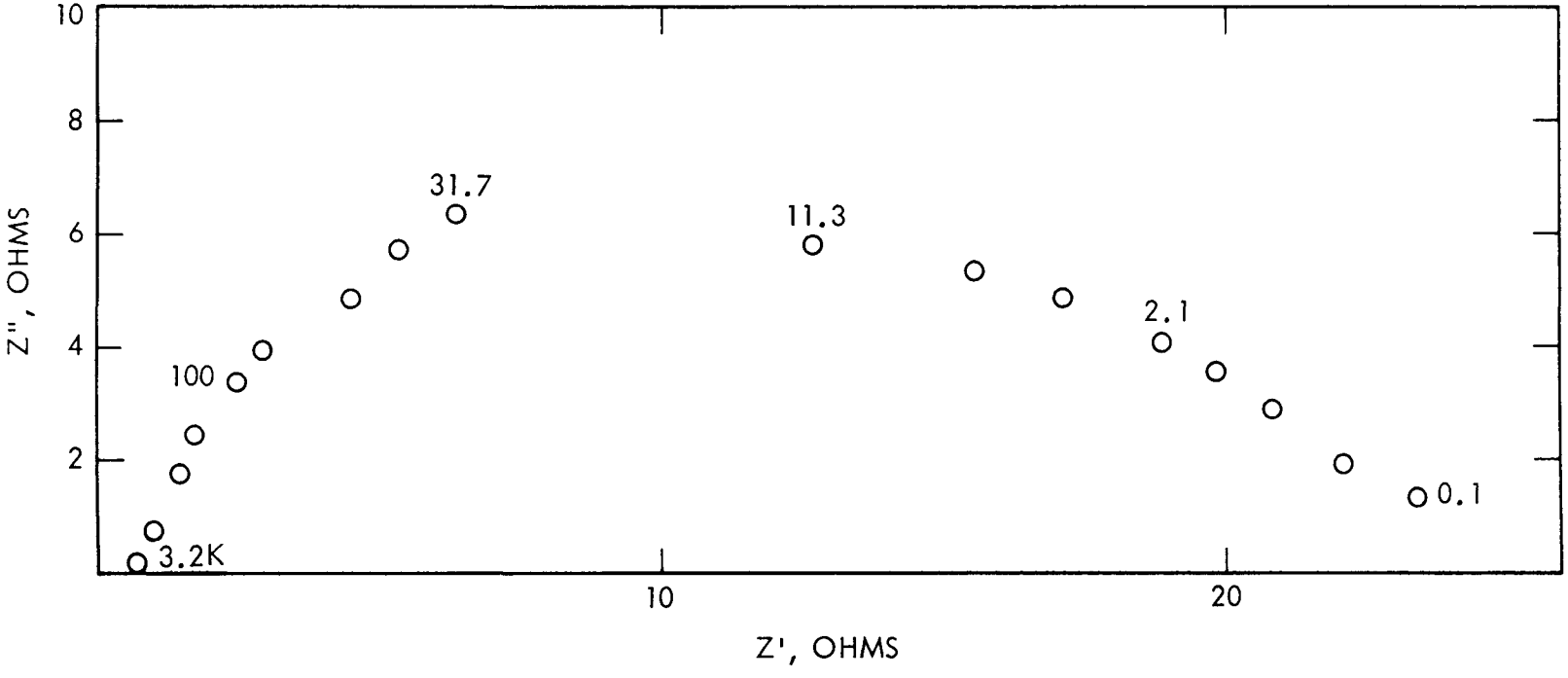

Figure 10: A.C. Impedance Data, Plotted on the Complex Plane, for a Good Performance (0.4 W/cm^2) Porous Molybdenum Electrode Free from Sodium Molybdate, Area = 4.01 cm^2, 1100 K, 1.5 Volts. Frequencies of Selected Points are Indicated.

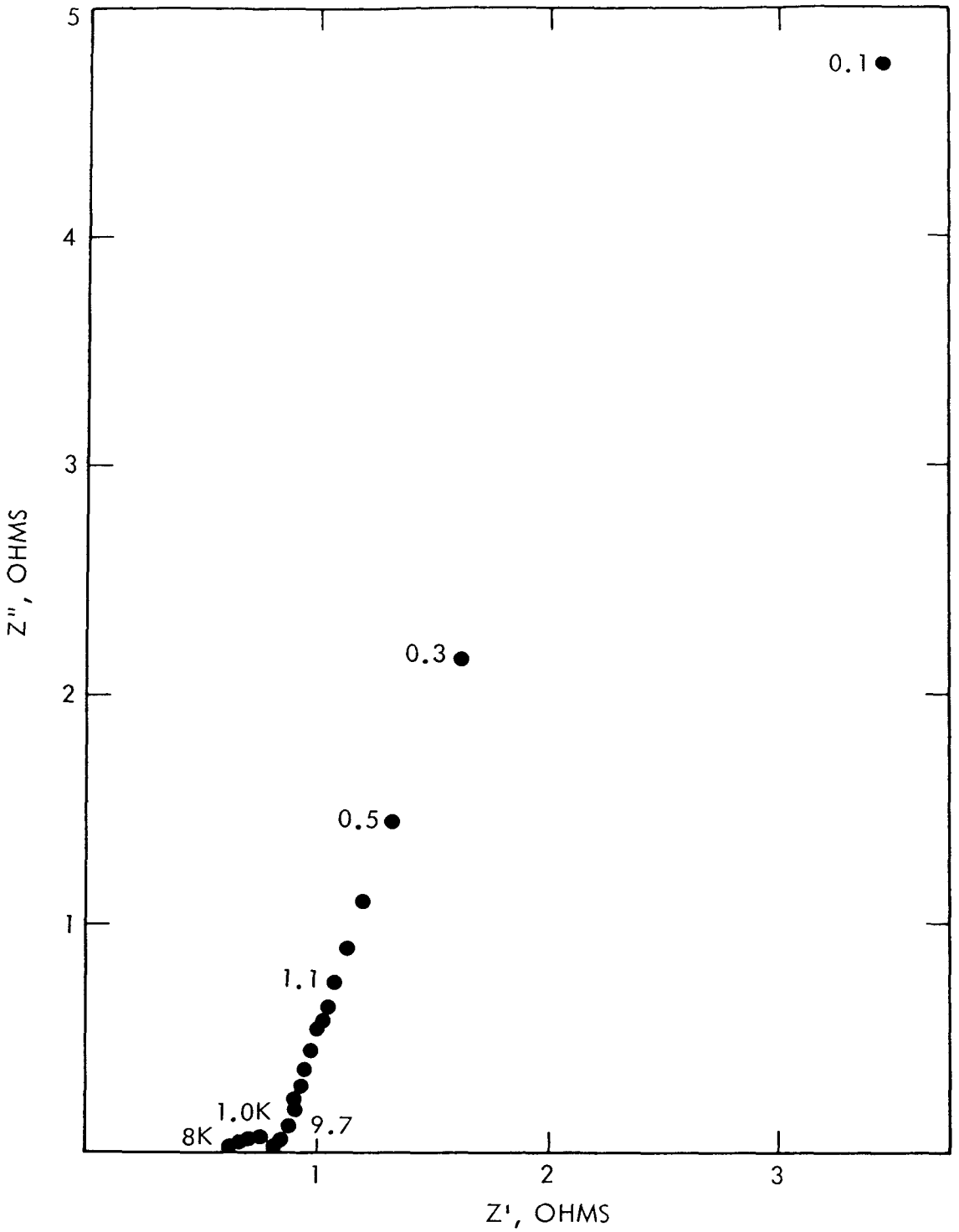

Figure 11a: A.C. Impedance Data, Plotted on the Complex Plane, for a Fresh Na_2MoO_4 Treated Molybdenum Electrode, Area = 4.71 cm^2, 1110 K, 1.5 Volt. Frequencies of Selected Points are Indicated.

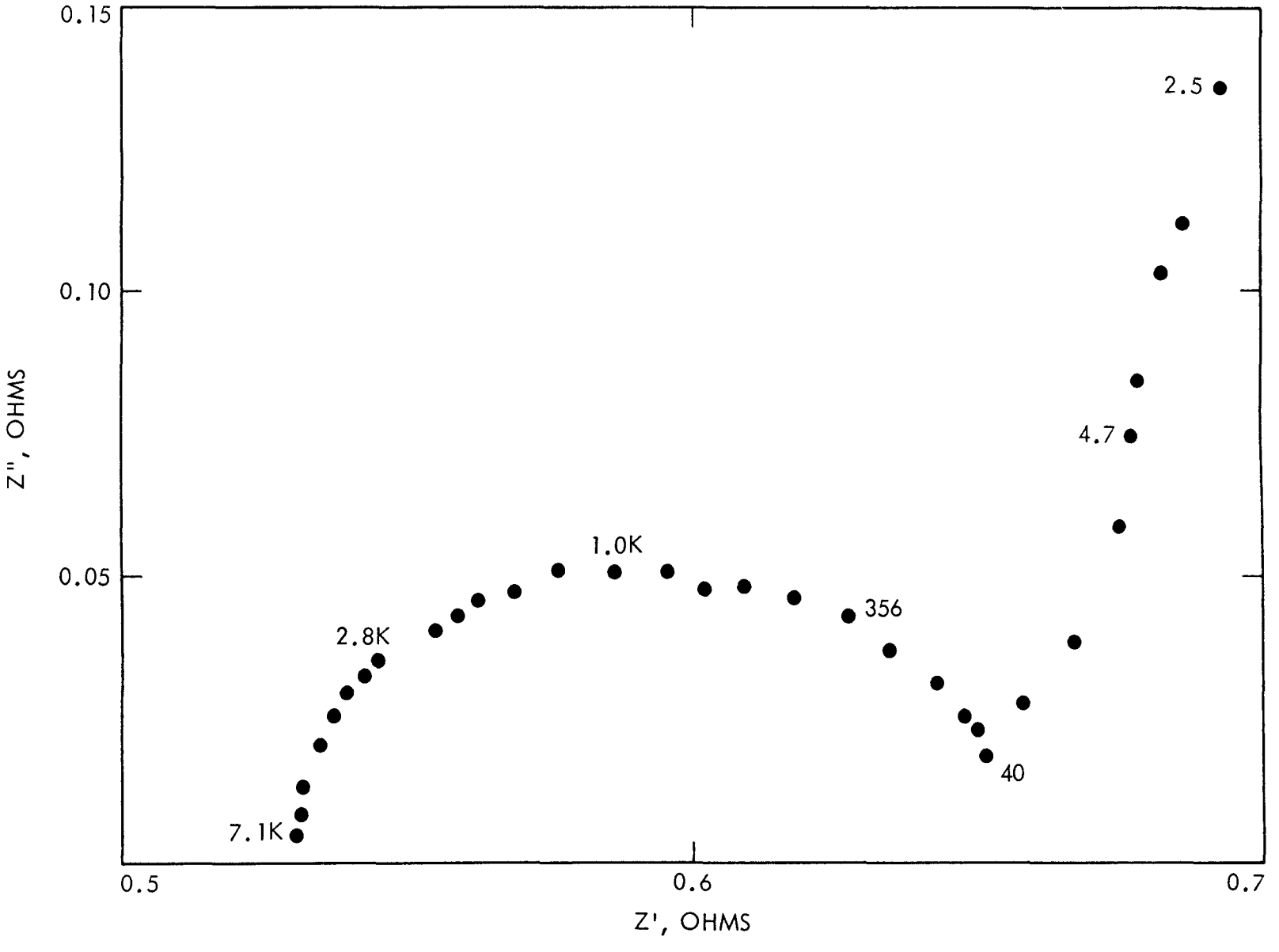

Figure 11b: High Frequency Loop, Due to Ionic Conduction and Capacitance of Na_2MoO_4, in an Undegraded Na_2MoO_4 Treated Molybdenum Electrode, Area = 4.71 cm^2, Grid Contact, 1080 K, 1.3 Volts.

total internal direct current resistance of the LMTEC cell. Instead it is actually the total resistance that exists in parallel to the bulk capacitance of the ionic conductors and, therefore, may contain contributions from the electrode in-plane ionic resistance as well as from normal-to-plane rersistances and BASE resistance. Note that the contribution of in-plane ionic resistance to the cell internal impedance in dc operation is negligible.

D. Conclusions

Deliberate addition of sodium molybdate to the Mo electrodes has a dramatic effect on the impedance behavior of the electrodes. Ionic transport within the electrodes dominates molecular diffusion resulting in a lower sodium back pressure within the electrode. This increases the cell voltage (decreases the charge transfer resistance) but slightly increases the total ionic resistance. Electronic resistance is increased due to corrosion of the metal. Loss of sodium molybdate occurs via evaporation in competition with corrosion of the metal electrode. Electrochemical cycling leads to corrosion at open circuit and recrystallization of the metal electrode at moderate-to-high current, giving rise to a modified electrode morphology. Eventually, loss of sodium molybdate, present in small concentrations in equilibrium with corrosion products, results in total depletion of oxide phases from the electrode. Sintering of the finely divided molybdenum then occurs, and eventually a near steady-state morphology is obtained. Vertical pores may be completely lost by this cycling, but porosity may increase and the effective area of the electrochemical interface between molybdenum, BASE, and vacuum may also increase. The degree to which each of these three processes occurs will determine whether the degraded, treated electrode

will be superior or inferior to an untreated electrode. In some cases, the degraded or mature state may have favorable morphological characteristics resulting in relatively high electrode efficiencies, if the electrode is subjected to small quantities of sodium molybdate. This may explain the performance of electrode #2, Figure 7, which was exposed only to sodium molybdate vapor. In any case, precise control of morphology and performance by sodium molybdate treatment would be difficult to achieve in practice.

V. VERY THIN MOLYBDENUM ELECTRODES

A. Introduction

The positive, current-collecting electrode in the LMTEC device must be a good electronic conductor to minimize efficiency losses due to i-R drop in this low-voltage, high-current device. Also, the electrodes should pose no resistance to sodium vapor away from the BASE. Thus, a very thin electrode would be desirable in connection with an overlying current collection grid. This would minimize flow resistance due to sodium vapor flow pressure drop, even in an electrode that has lost the sodium ionic conductor Na_2MoO_4 by evaporation. In addition, since part of the cause of degradation may be due to a change from the columnar morphology of the electrode to a less porous structure, a thinner electrode would be beneficial. Finally, an overlying current collection grid would be needed to offset the higher sheet resistance in a very thin film. The results of experiments utilizing very thin (<1 micron) Mo electrodes with current collection grids are presented in this section.

B. Experimental

Very thin Mo electrodes were prepared by magnetron sputtering of Mo onto a masked BASE tube in a method similar to that used to deposit thicker Mo electrodes (Section III). Seventy-five thin (0.13 mm) Mo wire strips were cut to the length of the electrode, laid on the tube longitudinally approximately 0.6 mm apart, and held in place by thicker Mo wires (0.5 mm diameter) in at least four places, as shown in Figure 12. A current and voltage probe was tied onto the electrode at the center with 0.5-mm Mo wire.

The length of the electrodes was approximately 1.5 cm. Since the

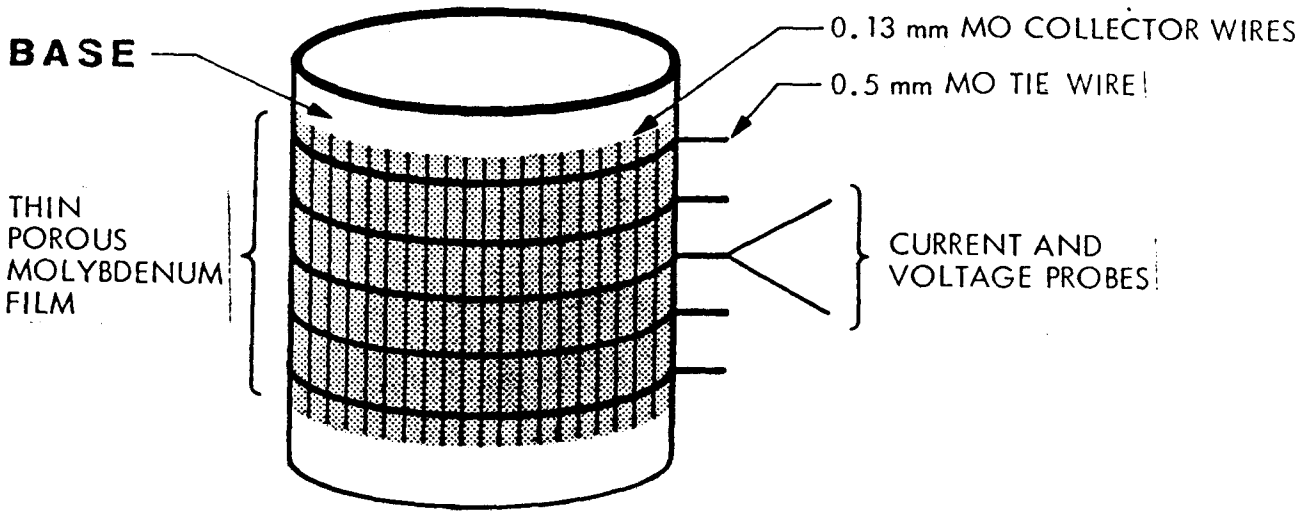

Figure 12: Schematic of Arrangement of Tied-On Molybdenum Current Collector Grid on Porous Electrode.

BASE tube has a diameter of 1.5 cm, the electrode areas were approximately 7 cm^2. In some cases the Mo wires were brazed to the electrodes as described in Section III. Sheet resistance measurements could be made on electrodes that had two to four current-voltage leads with no grids. The current was supplied with a power supply (Kepco model JOE 15 - 6 MVP, Flushing, NY) and monitored with a digital multimeter. The voltage was measured with a digital multi-function meter.

C. Results and Discussion

A compilation of sheet resistance measurement data is given in Table II for various thicknesses of Mo electrodes, both at room temperature and at LMTEC operating temperatures. The two-probe measurements include the contact resistances between the probes, the braze, and the electrode. Using the data from two-probe and four-probe measurements on the same electrodes, this resistance has been calculated to be on the order of 0.1 ohms per brazed contact. This is somewhat large and in an optimized device should be about 1 order of magnitude lower.

Accomplishment of this goal is not complex, and the contact resistance can be lowered by the use of more braze to approximately .03 ohms as has been observed previously with thicker electrodes. In the case of the very thin electrodes, however, braze was kept to a minimum in order to perturb less of the electrode area. Also, these braze connections are usually somewhat porous on inspection. Thus, further improvements in braze technology should reduce contact resistances with a more continuous, non-porous bond. Finally, the amount of braze used must not cover an excessive amount of electrode area. Further work is required to optimize these parameters.

At room temperature the sheet resistance is quite small until the

Table II

Typical Sheet Resistances

Molybdenum Electrodes

Nominal Thickness (μm)	Sheet Resistance at 300K (Ohms)	Sheet Resistance at AMTEC Operating Conditions 1000-1200K (Ohms)
0.15	62.2 four-probe	90,000 four-probe
0.30	2.65 four-probe	4,000 four-probe
0.45	2.67 two-probe	5.9 two-probe
0.5	1.38 four-probe	
0.6	1.12 four-probe	~60 four-probe
1.0	0.282 four-probe	
1.4	0.263 four-probe	0.98 four-probe
2.5	0.34 two-probe	0.42 two-probe

eletrodes are 0.5 microns or less in thickness. The actual point where the Mo film becomes discontinuous will depend on the surface roughness of the BASE tube and may vary somewhat from tube to tube. The high-temperature resistivities are significantly larger than the room-temperature data. This could be due in part to the positive thermal coefficient of resistivity of the metals involved and in part due to the sintering of the Mo film. The contact resistance was also observed to be at least twice the room-temperature value at the LMTEC operating range, so this may also be a contributing factor. The increase in contact resistance may be due in part to a poorer mechanical bond between the lead and electrode after temperature cycling, because of the difference in thermal expansion coefficients between the Mo wires and the BASE tube. A feature of possibly greater importance may be the fact that the dependence of braze resistivity on temperature will result in measured increases in contact resistance at high temperature.

The current-voltage curve characteristic of typical thin Mo electrodes with current-collecting grids is shown in Figure 13. These curves are not significantly different from either thicker Mo sputter-deposited films or films formed from Mo resinates. Thus, the current-voltage characteristics are relatively insensitive to morphology or thickness of the electrode. A very thin electrode without a collector grid will appear the same as one with a grid, except that the short-circuit current will be smaller. With the higher resistivity of very thin electrodes, the area surrounding the current collector that is effectively utilized will be smaller. Therefore, a very thin electrode must have a collector grid with a characteristic grid spacing that will optimize the effective area of the electrode utilized. Since these grids now appear to be very important, it is obvious that for maximum

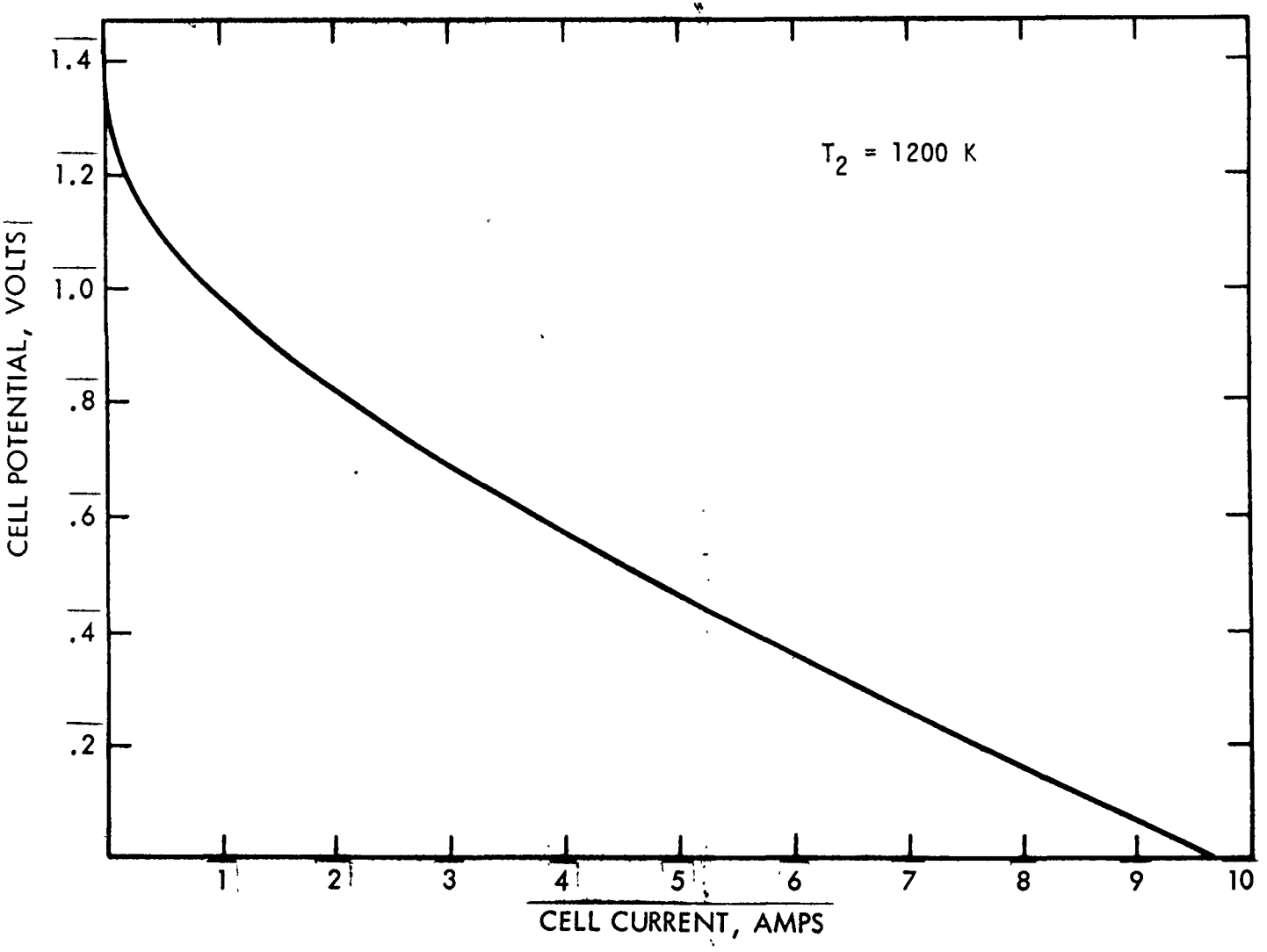

Figure 13: Current-Voltage Curve for 0.5 Micro Thick Molybdenum Electrode with Current Collector Grid (Grid: 1x2 mm, Electrode Area: 4.71 cm^2).

efficiencies to be obtained from very thin electrodes, the method for constructing collector grids must be dramatically improved. Work is currently underway in this area and modeling has recently been initiated to consider effective grid designs.

Higher power densities obtained with very thin Mo electrodes with collector grids can be expected from the reduced vapor diffusion resistance for sodium atoms and the collector grid offsetting the increase in sheet resistance of the thinner electrodes. Also, the degradation with time is much less dramatic for very thin electrodes compared with thicker Mo electrodes. Unlike the thicker electrodes which usually show decay in power density to 20 - 30% of the initial value over 100 hours (7), a 0.5-micron Mo electrode has a power density of 80% of the initial value after almost 100 hours (Figure 14). Thick electrodes (approx. 2 microns) initially contain greater quantities of sodium molybdate due to their greater pore surface area. Thus, a longer period of transport enhancement is expected, followed by significant degradation due to eventual sodium molybdate depletion. Also, thick electrodes may be slowly sintering from the porous, columnar structure they posses after deposition, to a more compact one. This could cause the resistance to atomic sodium vapor to further increase and an additional backing voltage to develop. Thinner electrodes, while still sintering with time, would not be expected to degrade as drastically, since the resistance to atomic flow is much lower. In the thickness range where the sheet resistance dramatically increases, the Mo film could be composed of interconnected islands, which would have significant pore volume between the islands. In this case, sintering of the Mo islands themselves would have a minimal effect on the sodium flow resistance. The effect of sodium molybdate in very thin electrodes will be minimized for two reasons; (a)

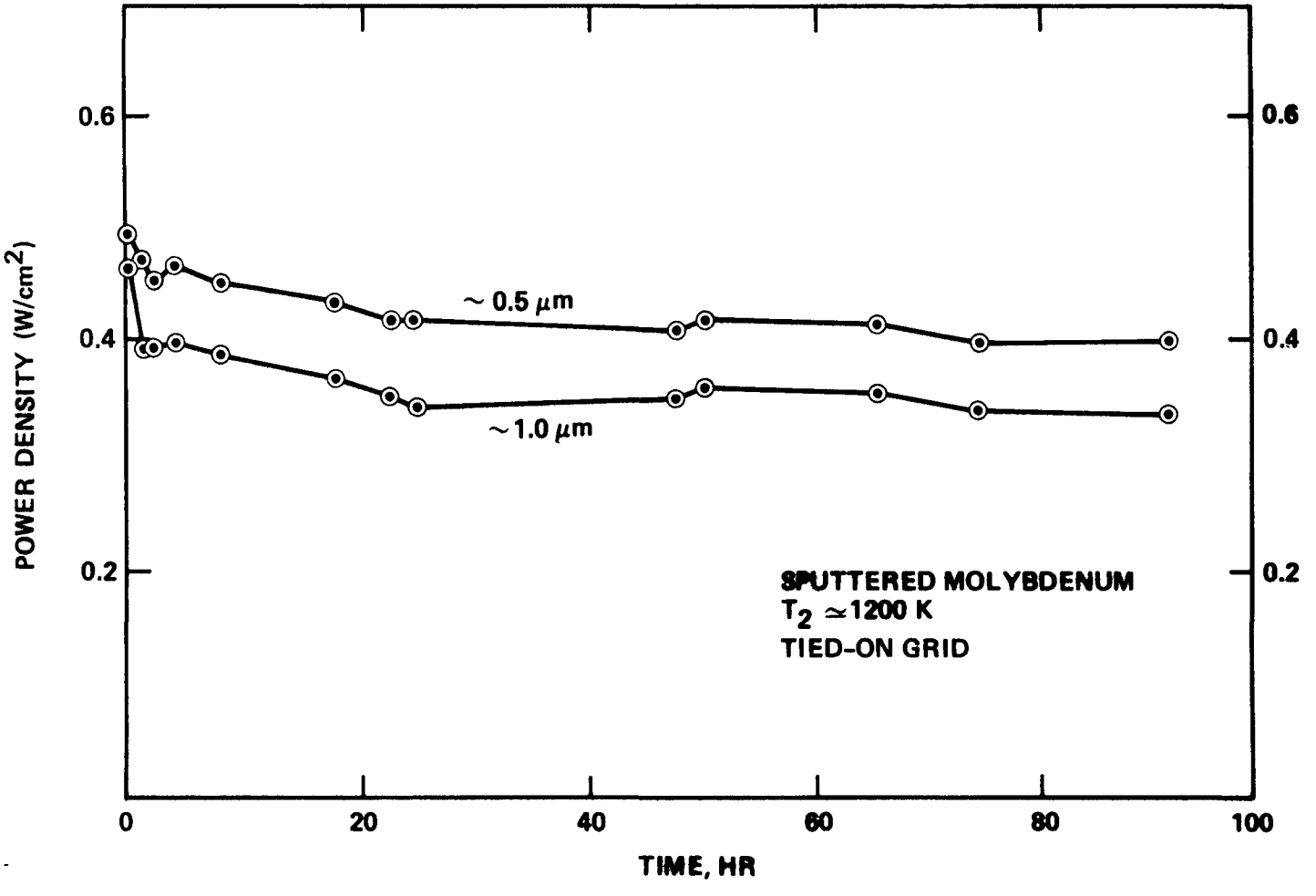

Figure 14: Power densities of thin, porous molybdenum electrodes with tied-on current collector grids.

less will be present to begin with and it will be lost quickly, and (b) its enhancing effect over pure sodium vapor flow will be less, since the vapor flow pressure drop has been substantially reduced.

Finally, thinner electrodes with grids are expected to be reproducible in deposition and more predictable in their performance, since sodium transport is not dependent on complex chemistry. Although comparable performance has been achieved with a thicker electrode (Figure 7, curve #2), that electrode was exposed both to sodium molybdate and oxygen during the test period, and the results were not replicated with other 2.5-micron Mo electrodes.

AC impedance experiments on these thin electrodes have allowed many features of the equivalent circuit to be determined. The ac impedance of one electrode at dc biases from open-circuit (approx. +1.25 V vs. Na) to near short circuit (approx. +0.1 V vs. Na) is shown in Figure 15. Because of the experimental arrangement in which the Na reservoir was grounded, the Mo electrodes were the counter and reference electrodes, and the Na was the working electrode in a two-electrode configuration. An equivalent circuit for the device can be determined from the impedance spectra. This circuit, shown in Figure 16, can be used to model electrode performance once the circuit components are resolved and quantified.

The resistance R_s is a combination of all resistances in the device that are in series with the other circuit elements. This includes lead resistance, contact resistance of the leads to the Mo film electrode, and part of the sheet resistance of the electrodes. This value was potential-independent, as expected for purely physical resistances, and had a value of approximately 1.0 $\pm$ 0.1 ohm. It is obtained from the high-frequency real axis intercept divided by the area of the electrode (by which the values have been normalized). The sheet resistance of the

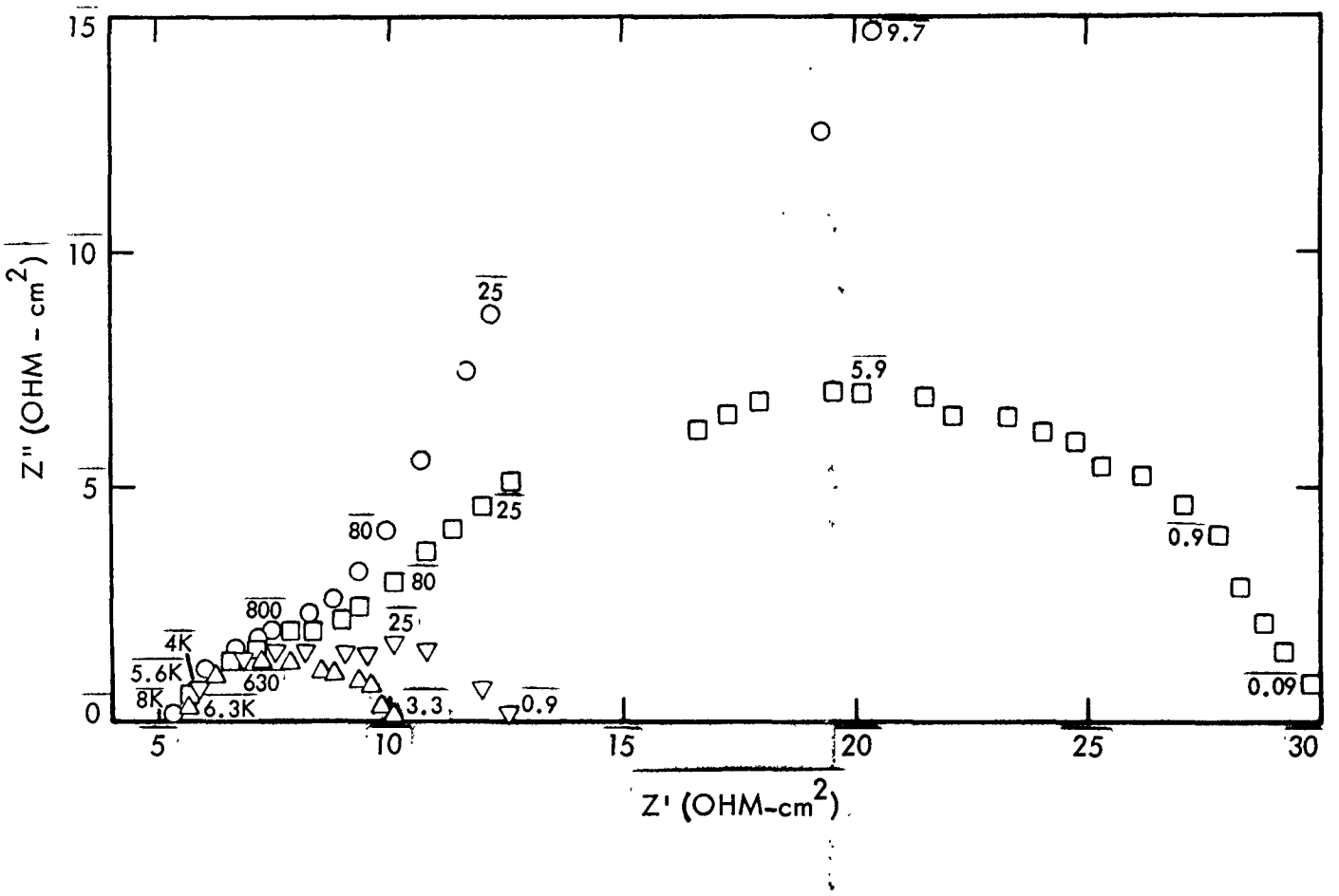

Figure 15: A.C. Impedance Data for a Thin (~0.6 Micron) Molybdenum Electrode at About 1050 K, Different D.C. Biases: ○, 1.2V; □, 0.8V; ▽, 0.4V; △, 0.1V. at 1.2V, a Maximum $Z'' \simeq 120$ OHM-cm^2 at 0.11 Hz, and the Extrapolated Low Frequency Real Axis Intercept is $Z' \simeq 375$ OHM-cm^2. Frequencies (in Hz) of Several Points in Each Data Set are Indicated by Numbers.

EQUIVALENT CIRCUIT DERIVED FROM COMPLEX IMPEDANCE MEASUREMENTS

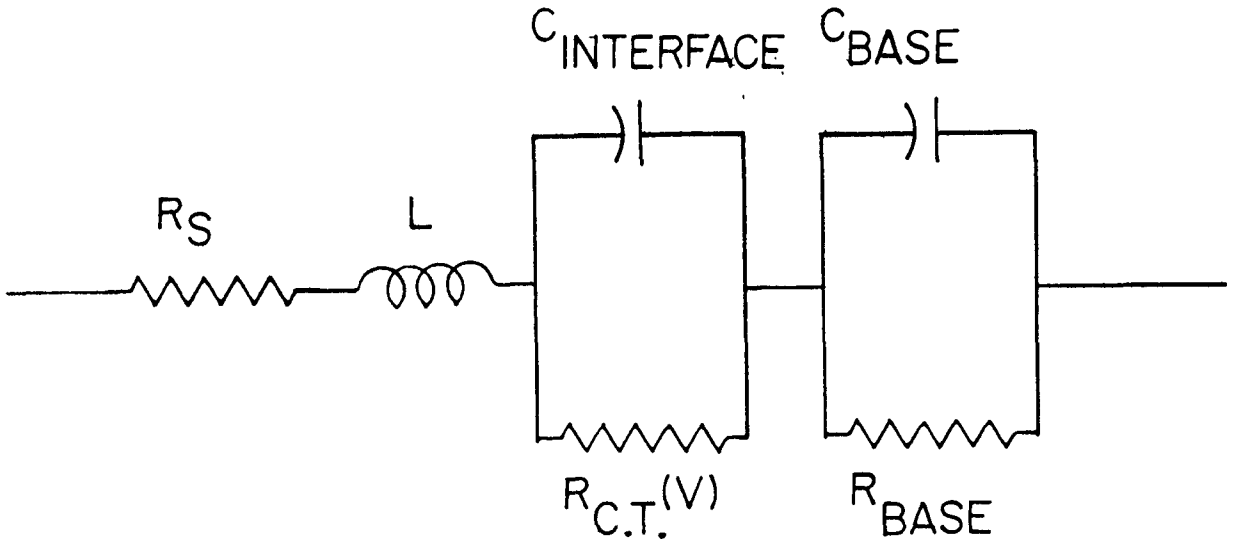

Figure 16. Equivalent circuit for LMTEC cell showing series resistance, R_s, and inductance, L, interfacial capacitance, C interface, and charge transfer resistance, $R_{c.T.}$, due to the porous electrode/BASE interface, and bulk capacitance, C_{BASE}, and resistance, R_{BASE}, of the solid electrolyte.

electrode can be thought of as a parallel combination of ever-increasing resistances as the distance from the contact increases. However, since it is a parallel combination, the equivalent resistance seen with the ac impedance experiment will, to a first approximation, be independent of the electrode sheet resistance. The higher the sheet resistance, the less of the electrode that will be effectively used.

The inductance is also a physical property and is caused by the ring-like nature of the contact and electrodes around the tube. Assuming a series inductance, the positive imaginary values can be fit to the expression $Z'' = 2 \pi f L$, where Z'' is the imaginary value of the impedance and f is the ac frequency. This value is calculated to be approximately 8 microH and is potential-independent, as one would expect. This value is too large to be caused by just the one coil of contact wire and is therefore probably a parallel combination of inductances from the electrode itself. The ac impedance spectra contain two loops that correspond to two parallel R-C combinations. The values of R can be determined from the diameter of the semicircle along the real axis. The value of C can be conveniently determined from $2 \pi f_o = (RC)^{-1}$, where f_o is the frequency of the values that lie at the top of the semicircle, and R is the resistance determined as just described. The values of R and C for the two loops are shown in Table III. It can be seen that the R for the first loop and both C values are independent of voltage, whereas the R for the second loop decreases toward short-circuit. As the time constant of the second loop approaches that of the first, the values of R and C become more difficult to extract and, therefore, more uncertain. The potential-independent first loop is most probably due to the BASE. However, it strongly depends on the history of the BASE tube and was often not detectable for fresh tubes with minimum exposure to air. The

Table III

R and C Values for Two Loops

VOLTAGE	1ST LOOP		2ND LOOP	
(V vs. Na)	$R(\Omega cm^2)$	$C(\mu F)$	$R(\Omega cm^2)$	$C(F)$
1.2	3.3	250	70	1.5×10^{-2}
0.8	3.3	310	19	8.2×10^{-3}
0.4	3.1	300	3.5	2.1×10^{-2}
0.1	3.5	370	2.4	4.8×10^{-3}

curcuit for the BASE has been shown previously (14) to include a non-Debye capacitance or a constant phase angle element that does not obey the usual relationship between the impedance of the capacitor and f^{-1}, but a relationship to f^{n-1}, where n has a value between 0 and 1. This has the effect of moving the center of the semicircle to negative values of Z". Both of the RC loops in the data shown here have centers that lie below the real axis. The second loop has an R that decreases as the faradaic current increases toward short-circuit, which is therefore assigned as a charge-transfer resistance. The slower heterogeneous charge transfer is probably the reduction of Na^+ at the Mo electrode. Therefore, the features that are visible by ac impedance are lead and contact resistances, electrode inductance, Na^+ ion transport through the BASE, and heterogeneous charge transfer at the Mo electrode.

D. Conclusions

Thin, porous Mo films show promise as collector electrodes in the LMTEC device. The thin films have reduced atomic sodium vapor flow impedance. The increased sheet resistance of the electrodes can be offset by the use of collector grids. The current-voltage behavior appears similar to the thicker M^o electrodes, but larger short-circuit current densities are obtained for mature electrodes. AC impedance spectroscopy can be used to obtain the resistances due to the contacts and leads, the inductance of the electrode, information about the Na^+ ionic transport in the BASE, as well as kinetic information about the reduction of Na^+ at the Mo electrode. However, ac impedance is not useful in detemining resistances in the thin Mo films.

Sheet resistance measurements show a large increase for thicknesses less than 0.5 microns. At a given level of grid pore size,

one thickness might be optimal. However, to obtain the ultimate power densities from the LMTEC device, refinements in the technique of placing collector grids on the electrodes will have to be achieved. This is one area in which work is continuing.

VI. NOBLE-METAL-BASED ELECTRODES

Noble-metal-based electrodes exhibit very promising properties, with power densities close to 0.6 W/cm^2, observed for both platinum/tungsten and rhodium/tungsten bilayer electrodes. Although a great deal of data indicative of chemical and morphological processes in these electrodes have been obtained, several different mechanisms of efficient electrode operation may be indicated and the nature of the dominant mode of sodium transport through the electrode has not been convincingly established. At the same time, it is also likely that optimum performance levels have not yet been achieved with these electrode systems. Initial experiments were carried out with electrodes prepared using inks as described in Section VII. Only the last experiment used magnetron sputtered platinum/tungsten bilayer electrodes, with tungsten between the BASE and a covering layer of platinum, with varying thicknesses of these layers. Extensive lifetime test data have not yet been obtained, but initial tests show fairly slow degradation after a small, rapid initial drop in power. The initial reasons for selecting platinum group metals for study are the following:

1. Chemical stability: Attack of platinum metals on BASE is thermodynamically very unfavorable due to the low stability of their oxides.

2. Ruggedness: All platinum group metals except palladium are very non-volatile, comparable only with early transition metals, boron, carbon, and several actinides.

3. Possible compound formation with sodium: Alloying with sodium could lead to enhanced sodium transport by a non-gas- diffusion mechanism such as enhanced surface diffusion or diffusion through a liquid alloy.

Evidence for reaction of sodium with platinum exists in the literature. Other favorable characteristics of platinum group metals include low resistivities, especially of rhodium (4.5 micro-ohm-cm) and iridium (5.1 micro-ohm-cm), and thermal expansion coefficients that are slightly greater than those of the BASE. This might allow tailoring of the thermal expansion coefficient of an alloy or composite with molybdenum or tungsten, which have thermal expansion coefficients lower than that of the BASE.

Figure 17 shows the current voltage curves for a number of better performing electrodes of several varieties for comparison. The electrodes made of W/Pt, Mo/Na_2MoO_4, and W/Rh, labeled [a:], [b:], and [C:], respectively, in Figure 17 are at the beginning of life. The electrode labeled [d:] is one of the best examples of a high-performance, degraded (or mature) molybdenum electrode. It has lost nearly all Na-Mo-O phases, exhibits flat power density vs. time behavior (at 90 hours) and exhibits a current density close to zero at 1.35 V. The other electrodes all show current densities of about 20 mA/cm^2 at this voltage. This part of the power curve is not strongly affected by either electronic sheet resistance or the ionic conductivity of the BASE. These latter resistances give a much more shallow slope, characteristic of the high-current portion of the curve, than is observed near open circuit. Electrodes [a:], [b:], and [c:] show open-circuit voltages close to 1.5 V vs. sodium.

The difference in behavior can be explained by a rapid increase in sodium activity (sodium back pressure), or comparatively slow charge-transfer kinetics in electrode [d:]. The other electrodes necessarily have both efficient charge-transfer kinetics and exhibit an efficient mode of sodium transport to the electrode surface. The

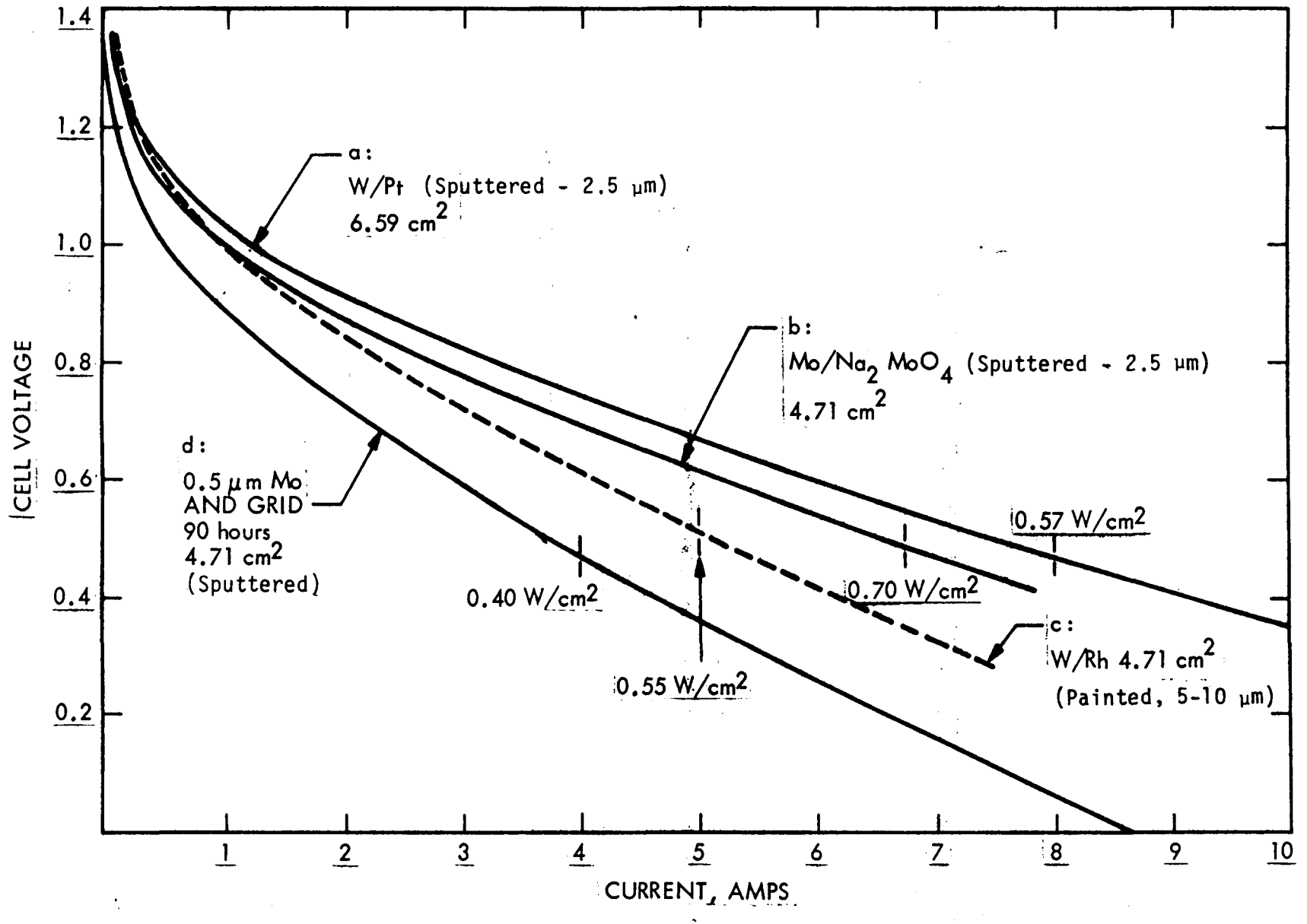

Figure 17: Current-Voltage Curves for Several High Performance Electrodes.

magnitude of the current densities at higher voltages is a sensitive indication of the efficiency of the sodium mass transport through the electrode. It is apparent that Pt/W and Rh/W electrodes provide such an efficient mode of transport that they compare favorably with the Mo electrode containing Na_2MoO_4, labeled [b:] in Figure 17.

Figure 18 shows the power densities vs. temperature for electrodes composed of W, Rh, Pt, W/Pt, and W/Rh. Clearly, the two-component, bilayer electrodes exhibit properties unlike either of their components alone. The break in the power vs. temperatue curves for Rh and Pt was ascribed to major morphological changes in the electrode due to melting or sintering, based on post-mortem analysis. After cool-down, it was found that these electrodes had coalesced into small, generally isolated droplets and puddles with only a fraction of the original electrode material, and area, in electrical contact with the contact lead. Initially, all these electrodes had a fairly homogeneous, porous appearance to their films.

The possibility that melting of these electrodes had formed platinum sodium and rhodium sodium alloys provided impetus to study these electrodes with morphology-stabilizing underlayers consisting of metals such as W or Mo. Work at Ford Motor Co. research laboratories had demonstrated that the liquid electrodes, Sn and Sn/Zr, were capable of operation at high-power densities (12). Although the high rate of Sn evaporation at LMTEC operating conditions makes these electrodes impractical for actual devices, they are highly informative models for studies of electrode properties. Sn/Zr liquid metal electrodes showed some of the best results ever obtained for LMTEC electrodes with power densities of about 0.50 W/cm^2 obtained after operation for 140 hours. These results make a non-volatile liquid alloy a very promising target for

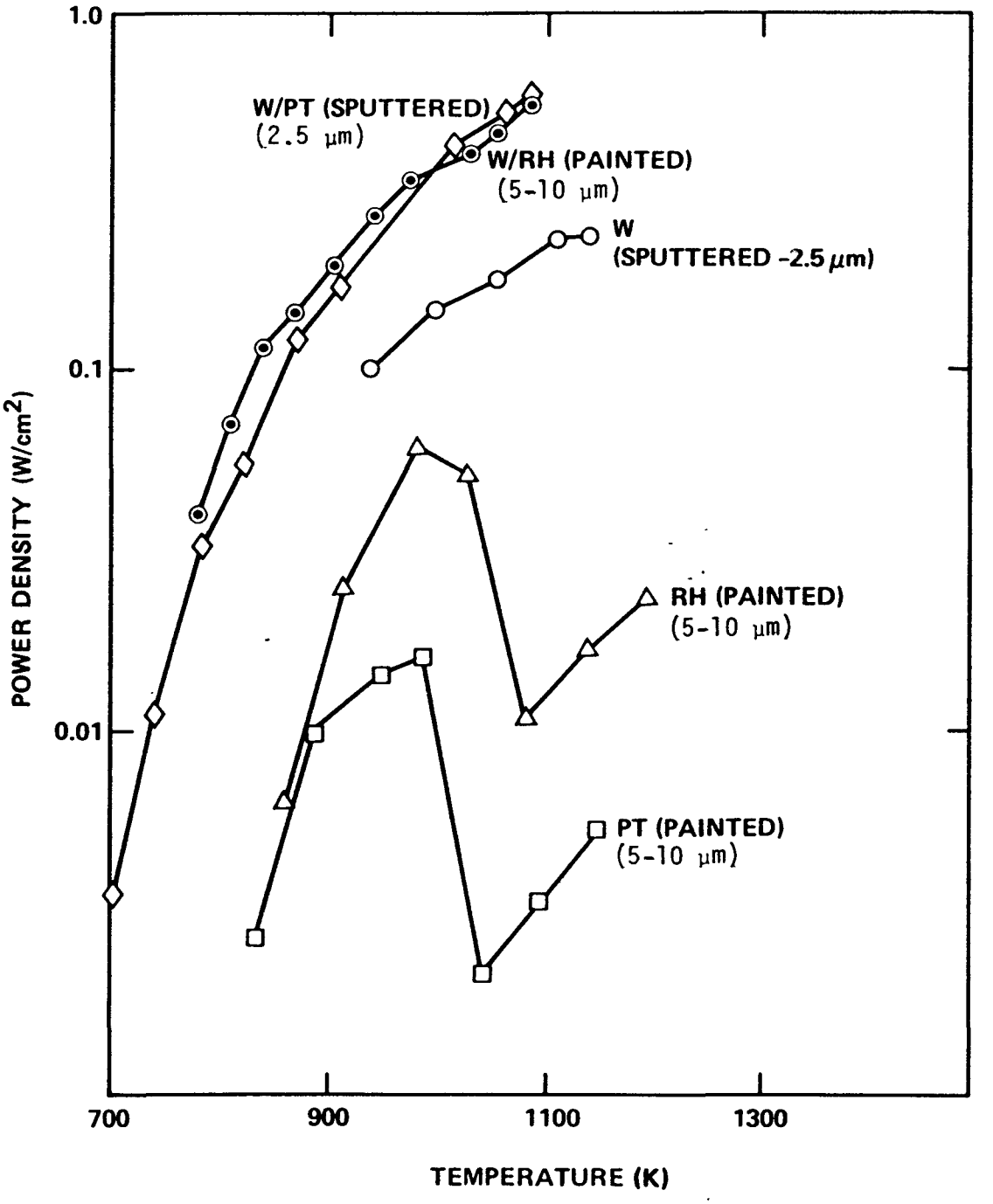

Figure 18. Power Density vs. Temperature for High-Performance Electrodes.

LMTEC electrode research.

Convincing evidence of sodium-platinum compound formation was obtained by reacting platinum with a large excess of Na in a sealed Ta tube and slow cooling from 1000 K to 525 K. The tube was then cooled and removed from its stainless steel evacuated container in an argon filled glove box, opened, and reheated to over 373 K to remove excess, molten Na. The remaining contents of the tube were etched with alcohol to reveal small, metallic black, flat platelets. The x-ray powder pattern of this material has been obtained as well as Laue photoghraphs that indicate hexagonal or rhombohedral symmetry. The stoichiometry is unknown, since the sample was found by XRD to contain some very finely dispersed platinum, probably produced by the etch, along with the more highly crystalline platinum-sodium alloy.

No extended lifetime data on good-quality, low-sheet resistance W/Rh or W/Pt electrodes have been obtained. The sputtered W/Pt electrodes were held at operating temperature (1050 - 1080 K) for 18 hours before tube failure led to abortion of the experiment. (Failure of the tube is ascribed to the fact that the tube was "recycled" from a previous experiment by washing in alcohol and grit-blasting the exterior surface. Tubes treated in this way have a greater tendency to fail due to prolonged handling and atmosphere exposure). The power densities for these electrodes are shown in Figure 19. These electrodes were at least comparable with state-of-the-art Mo electrodes in the first 20 hours of operation and will be considered further in longer lifetime studies since very few other compositions, with the exception of Mo, perform as well. Electrodes labeled A and B in Figure 19 were found to easily deadhere from the BASE on post mortem while the electrode labeled C was still fairly adherent. No Na-Pt was detected in electrodes on post mortem, but this

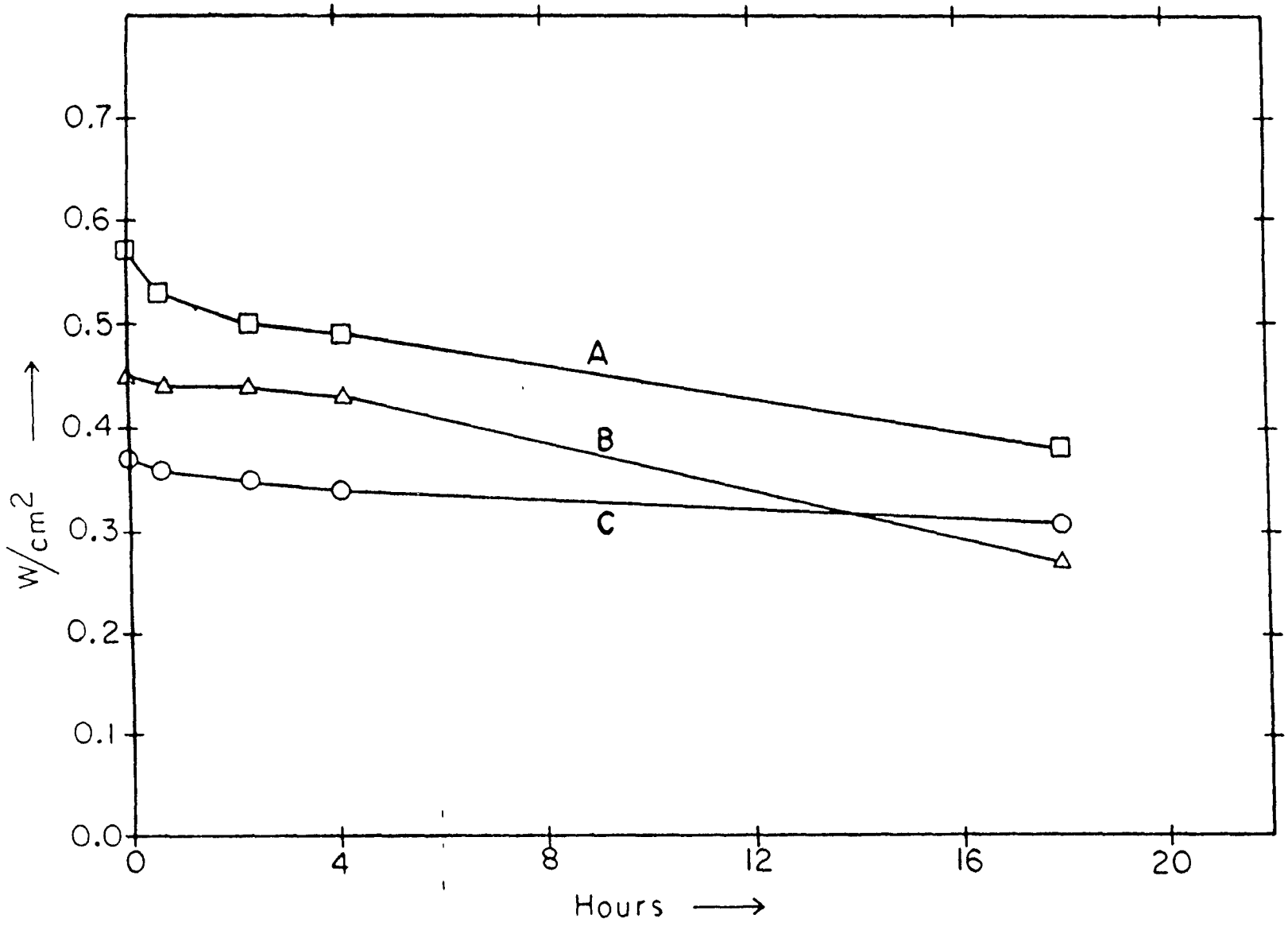

Figure 19: Maximum power vs. time for three platinum/tungsten bilayer electrodes:
A - 1.4 μm W/0.4 μm Pt, 1080K; B - 0.8 μm W/1.0 μm Pt, 1080K;
C - 0.4 μm W/1.4 μm Pt.

phase may not be stable except during discharge of the cell when sodium pressure at the electrode is high. Both Pt and W, as well as very small quantities of sodium tungstate, Na_2WO_4, were detected by XRD. At this point, it is not possible to resolve the question of the origin of the enhanced Na transport in W/Pt electrodes--either Na-Pt or Na_2WO_4 or a combination of both could play a role. Further studies on these systems are in progress.

XRD studies of W/Rh electrodes following operation as LMTEC electrodes reveal diffraction lines due to substantial quantities of elemental W, traces of Na_2WO_4, little or no elemental Rh, and a large number of unidentified lines. Alloys of Rh with Na, W, or combinations of them have not been ruled out. Further, studies of noble metal-based electrodes should address the nature of the Na transport mechanism; the stoichiomeetry, structure, and thermodynamic properties of sodium-noble-metal alloys, which may form in the electrodes; the influence of electrode morphology (consecutive layers or co-sputtered, homogeneous films); and further study of the Rh/W system. In addition, replacement of the noble metal by its eutectic formed with a metalloid (Si or Ge) would lead to a known liquid alloy worth investigating for high-power LMTEC applications. Pt-Si, Au-Si, and Au-Ge are all known to form eutectics that are liquid within the LMTEC operating regime.

VII. OTHER ELECTRODES AND DEPOSITION TECHNIQUES

A variety of other electrodes and deposition techniques has been investigated in order to identify promising alternatives to sputtered porous Mo. Systems that could be expected to exhibit efficient modes of condensed-phase Na transport were selected, with further requirements of chemical and morphological stability in the LMTEC electrode environment. Simple deposition techniques, suitable for testing a variety of electrode compositions, were also developed in order to facilitate this work. Inks (metal resinate inks, Engelhard Corp.) were used to prepare Mo, Rh, Pt, W, W/Rh, W/Ir, and W/Pt electrodes on BASE tubes. In general, good-quality, low-resistance electrodes could readily be obtained with all inks except Mo resinate, which often gave high-resistance films. Rh and Pt did not adhere well unless several very thin layers were applied and cured in succession.

The noble metals adhered fairly well to W films. Engelhard inks used were #8826, 10% Rh; #9450, 26% Pt; #1123, 6% Ir; #8605, 13.3% Mo; #8629, 22.2% W. The procedure used to apply them was to paint coatings as thinly as possible (2 - 3 microns) on the tube, dry them with a heat gun to obtain a hard, non-tacky film, and repeat the process until three to five layers had been deposited. Subsequent curing in air yielded films of varying porosities and thicknesses depending on the ink used. The Mo inks generally resulted in low porosity, yellow films estimated to be about 5 - 10 microns thick of MoO_3 after curing at 725 - 750 K. Tungsten inks resulted in more porous, powdery, yellow-green films with a thickness estimated 10 microns of WO_3 after curing at 825 K. Platinum and rhodium inks produced porous black and grey films respectively, both less

than 5 microns thick after curing at 675 K. The performance characteristics of noble metal-based electrodes were discussed in the previous section. It was found to be critically important to slowly increase the temperature during curing. The films of MoO_3 and WO_3 were subsequently reduced at 990 - 1040 K under dry hydrogen gas for four hours to yield porous metallic films 3 - 5 microns thick. The W films routinely exhibited sheet resistances of about 1.0 ohm/square, but the best Mo films gave resistances of about 3.0 ohm/square and often exhibited much higher sheet resistances, which in some cases increased with time.

An improved technique of preparing Mo electrodes and Mo-ceramic electrodes was developed in order to eliminate the complex procedure used for obtaining Mo electrodes from inks. Molybdenum trioxide was directly applied to the BASE tubes as a slurry in Nicrobraze 400 cement by spray painting. The slurry consisted of 10 ml of cement, 10 ml of acetone, and 15 g of reagent-grade powdered MoO_3. Similarly, slurries of MoO_3 and BASE powder in the cement could be painted onto the BASE tubes. No curing step in air or oxygen was necessary for these cement-based electrodes. The tubes were simply heated under dry hydrogen gas to at least 975 K for 1-1/2 - 4 hours. This procedure was found to completely decompose the Nicrobraze cement into volatile compounds without the need for an oxidation step as in the resinate inks. This procedure is less likely to result in possible harmful side reactions such as:

$$(3n + 1)\ MoO_3 + Na_2O\ (Al_2O_3)_n \Rightarrow Na_2MoO_4\ \ nAl_2(MoO_4)_3, \qquad (3)$$

since the tube and electrode precursor material will only be heated under reducing conditions. MoO_3 is reduced, first to oxygen-deficient materials, MoO_{3-x}, then to MoO_2 at temperatures substantially below

the temperature range where reduction to Mo metal occurs.

Molybdenum/BASE cermet electrodes about 10 - 15 microns thick were prepared as described, but were subsequently annealed at 1370 K under argon/hydrogen to sinter the electrode. The cermet (68w% Mo/32w%BASE) exhibited a sheet resistance of 45 ohm/square at room temperature and 23 ohm/quare at 1000 K with a rather poor power density of 0.04 W/cm^2 drawn from two leads, each with contact length of 4.7 cm at 0.4 and 1.5 cm across a 1.9-cm tall electrode (8.95 cm^2).

These electrode fabrication techniques are less reproducible and provide lower performance electrodes than does magnetron sputtering. However, the technique for fabrication of cermets is a useful tool, since these materials cannot, in general, be prepared by sputtering. Although poor results were obtained initially with cermets, these electrodes have promise. Ford Motor Co. researchers have obtained power densities of 0.5 W/cm^2 after 150 hours using similar techniques (16). Using flame spray deposition techniques the Ford researchers have achieved close to 0.3 W/cm^2 after 40 hours and 0.16 W/cm^2 after 134 hours (12). These electrodes should exhibit great durability over long lifetimes. Improvements might be achieved with the use of an efficient current collector (e.g., a grid) embedded in the cermet. Also, a dramatic improvement could be achieved if a BASE with significant electronic conductivity and stability in the LMTEC environment could be synthesized. Fundamental research addressing the possibility of substituting transition metal ions into the "spinel block" of beta-and beta"-aluminas to enhance electronic conductivity is currently in progress.

VIII. RECIRCULATING TEST CELL

A Recirculating Test Cell (RTC) is essential for conducting long-term testing of electrodes without having to disturb the test cell system in order to replenish the liquid metal. As part of this contract, an RTC was designed (Figure 20) with the intent of performing long-term testing of electrodes. The RTC shown in Figure 20 is an externally heated configuration without an internal heater well and is designed to fit into a standard tube furnace for testing. This design is intended to simplify sodium reservoir heating when thermal calorimetry is not being carried out, and allows investigation of remote condenser concepts. Although the system has not yet been fully assembled, the hot section consists of a 1-1/2 inch id stainless steel tube sized to fit into a 32-cm long tube furnace capable of temperatures in excess of 1300 K. The sodium reservoir contained in the BASE tube will be heated by radiation from the hot outer wall to the surface of the BASE tube. The RTC will be mounted vetically in the tube furnace with the condenser extending out the bottom. The condenser will be thermally isolated by a 3/4-inch, thin-walled bellows between the hot section and the condenser. Sodium vapor will flow down along the hot section tube, through the bellows, and into the condenser. The top flange contains two electrical feedthroughs capable of carrying approximately 50 A each. Thus, two electrodes (approximately 25 cm^2) can be tested simultaneously. The sodium feed line, a gas vent, and a thermocouple well will enter the containment vessel via a 3/4-inch stainless steel tube, which will also support the BASE tube. The BASE tube will be demountable and attached to the support tube by a modified miniconflat flange. At the present time the acquisition of parts to assemble the RTC has begun. Further progress is pending further funding.

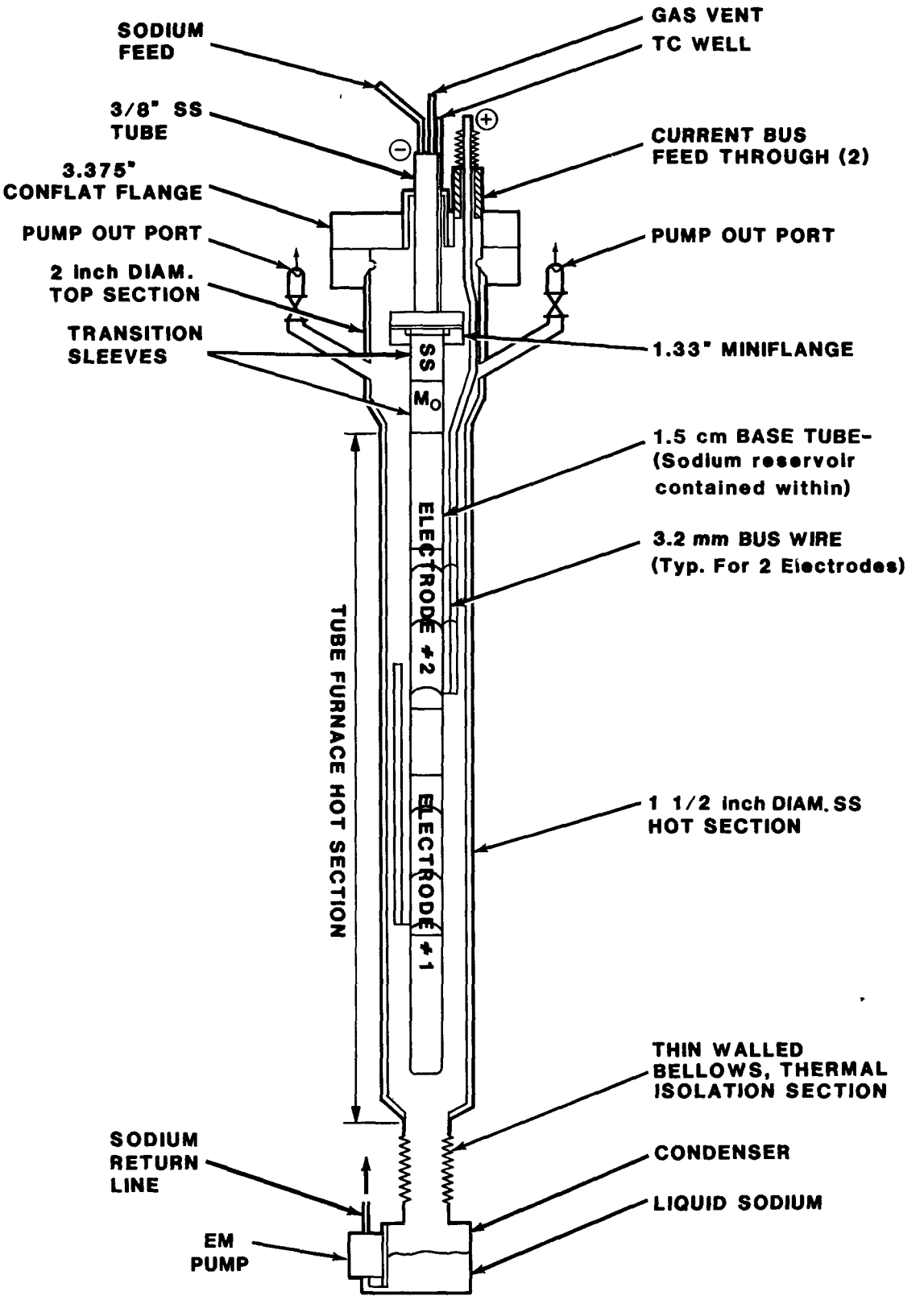

Figure 20. Externally Heated LMTEC RTC.

IX. SUMMARY OF CONCLUSIONS

Experimental work on LMTEC electrodes has continued to show significant progress toward the development of long-life, high-power electrodes. The major conclusions resulting from the work described in this report are

(i) Direct application of Na_2MoO_4 to fresh and/or degenerated Mo electrodes results in enhanced sodium transport and, therefore, LMTEC performance. Thus, Mo electrodes might be regenerated during the lifetime of a LMTEC cell. However, corrosion reactions and evaporation result in an increase in electronic sheet resistance and an irreversible loss of metallic Mo. It is estimated that periodic regeneration of Mo electrodes could extend LMTEC high-power operation to more than 1000 hours, but not more than 5000 hours. The ultimate lifetime under these circumstances must be detemined by LMTEC testing under load, since Na_2MoO_4 is electrochemically stable at maximum power conditions. Most lifetime data to date have been taken with LMTEC cells on stand at open circuit and high temperature, with periodic voltage vs. current scans being taken every few hours.

(ii) Very thin (<1 micron), porous Mo films show promise as collector electrodes in a LMTEC. These very thin electrodes would not require Na_2MoO_4 to enhance the sodium flow, since vapor flow impedance is significantly reduced. The increased sheet resistance of the electrodes can be offset by the use of collector grids. Results in this report show that very thin Mo electrodes may be able to produce more than $0.5W/cm^2$ for long periods (possibly thousands of hours) since no

chemical or physical degradation mechanisms are yet apparent. Optimization of the electrode/grid configuration is needed.

(iii) Noble-metal-based electrodes also exhibit very promising properties, with initial power densities close to 0.6 W/cm^2 exhibited by both Pt/W and Rh/W bilayer electrodes. No long lifetime data have been obtained for these compositions, and the mechanism of Na transport is not yet known. Work is continuing on these compositions.

(iv) Magnetron sputtering of thin metallic films continues to be the most favored method for depositing high-power LMTEC electrodes. Other deposition techniques using inks and slurries have not been practical to date for durable, high-power operation. Further work is needed in this area.

(v) Initial investigations of cermet electrodes indicate that their performance will be very sensitive to composition and deposition techniques. Considerable research and development will be necessary to produce even a moderate power cermet electrode. This is confirmed by work at the Ford Motor Co. on cermets (16), since the 0.5 W/cm^2 stable power electrode achieved was never reproduced.

(vi) Significant work remains to be done in the electrode development area for any LMTEC intended for long lifetime applications. A salient feature of the LMTEC, which makes it ideal for remote, solar-heated applications, is the minimal maintenance required. For an electrode to be able to complement these requirements, it must be able to perform without alterations an average of 60,000 hours. Furthermore, the requirements for the solarized LMTEC design require the application of the electrode on the interior of the BASE tubes since this is the ideal situation when metals other than sodium with higher vapor pressures at the intended operating conditions require the inherently higher structural

characteristics of the BASE tubes in compression. Limited work on applying a metal electrode on the interior of BASE tubes is currently in progress at Sandia.

XI. REFERENCES

1. N. Weber, "A Thermoelectric Device Based on Beta-Alumina," Energy Conversion 14:1, 1974.

2. T. Cole, "Thermoelectric Energy Conversion with Solid Electrolytes," Science 221(4614):915, 1983.

3. T.K. Hunt, N. Weber, and T. Cole, "Research on the Sodium Heat Engine," Proceedings of the 13th Intersociety Energy Converison Engineering Conference, SAE, Warrendale, PA, p. 2011, 1978.

4. T.K. Hunt, N. Weber, and T. Cole, "High Efficiency Thermoelectric Conversion with Beta"-Alumina Solid Electrolytes, The Sodium Heat Engine," Fast Ion Transport in Solids, ed. J. B. Bates and G. C. Farrington, North Holland Publishing Co., Amsterdam, p. 263, 1981.

5. H.L. Chum, and R.W. Osteryoung, Review of Thermally Regeneratived Electrochemical Systems, SERI Report TR-332-416, Vols. 1 and 2, April 1982.

6. C.P. Bankston, T. Cole, R. Jones, and R. Ewell, "Experimental and Systems Studies of the Alkali Metal Thermoelectric Converter for Aerospace Power," J. Energy 7(5): 442.

7. C.P. Bankston, T. Cole, S.K. Khanna, and A.P. Thakoor, "Alkali Metal Thermoelectric Conversion (AMTEC) for Space Power Systems," Space Nuclear Power Systems 1984, M. S. Genk and M. D. Hoover eds., p. 393, Orbit Book Co., Malabar, FL, 1985.

8. "Alkali Metal Thermal Electric Converter: Preliminary Assessment for Railway Locomotion," prepared for Burlington Northern Railroad by Teknekron, Inc., Berkeley, CA, April 1983.

9. K. Subramanian and T.K. Hunt, "Solar Thermal/Electric Power Conversion Using the Sodium Engine," ASME Solar Energy Conference, April 1983.

10. K. Subramanian and T.K. Hunt, "Solar Residential Total Energy System Using the Sodium Heat Engine - A Concept Study," Proceedings of the 17th Intersociety Energy Converison Engineering Conference, IEEE, New York, p. 1474, 1982.

11. L.L. Lukens, "LMTEC Technology Assessment and Development," presented at the AMTEC Workshop, Jet Propulsion Laboratory, Pasadena, CA, April 24, 1986.

12. T.K. Hunt, Research on Materials Related to the Sodium Heat Engine: Final Report, Report No. LBL-21232, Lawrence Berkeley Laboratory, Berkeley, CA, March 1986.

13. T.K. Hunt and N. Weber, Ford Scientific Research Staff, private communication, 1986.

14. H. Engstrom, J.B. Bates, W.E. Brundage, and J.C. Wang, "Ionic Conductivity of Sodium Beta"-Alumina," Solid State Ionics 2(265), 1981.

15. B. Dunn, R.M. Ostrom, R. Seevers, and G.C. Farrington, "Divalent Cation Conductivity in Beta"-Alumina," Solid State Ionics 5(203), 1981.

16. T.K. Hunt and N. Weber, "Research and Development Program on a Sodium Heat Engine," Final Report for the period January 1979-September 1982, U. S. Department of Energy Contract No. DE-AC02-79ER10347, Ford Motor Co., Dearborn, Michigan, October 1982.

17. M.W. Breiter, N.S. Choudhury, and E.L. Hall, "Anodic Degradation of Beta"-Alumina in Contact with Mercury," J. Electrochemical Society 133(10): 2064, 1986.

Distribution:
0400 R. P. Stromberg
1510 J. W. Nunziato
1513 D. W. Larson
1820 R. E. Whan
1824 J. N. Sweet
1840 R. J. Eagan
1841 R. B. Diegle
1842 R. E. Loehman
1846 D. H. Doughty
2520 N. J. Magnani
2525 R. P. Clark
2540 G. N. Beeler
2541 J. P. Abbin
3141 S. A. Landenberger (5)
3151 W. L. Garner (3)
3154-3 C. H. Dalin - DOE/OSTI (8)
3160 J. E. Mitchell
6000 D. L. Hartley
6200 V. L. Dugan
6220 D. G. Schueler
6221 E. C. Boes
6222 J. V. Otts
6223 G. J. Jones
6224 D. E. Arvizu
6225 H. M. Dodd
6226 J. T. Holmes
6227 J. I. Martinez (10)
6227 J. A. Leonard (20)
6210 B. W. Marshall
6211 B. Granoff
7470 J. L. Ledman
7471 D. L. Stewart
8524 P. W. Dean
8470 R. L. Rinne
8471 A. C. Skinrood